FAILURE ASSESMENT DIAGRAM

ON LOW TEMPERATURE OF 20MnMoNi55 STEEL

Thesis submitted in partial fulfilment of
the requirement for the degree of

MASTER of NUCLEAR ENGINEERING

By

ANIL KUMAR PANJA

Examination Roll No: M4NUE19002

Registration No: 141079 of 2017-2018

Under the Guidance of

Dr. SANJIB KUMAR ACHARYYA

DEPARTMENT OF MECHANICAL ENGINEERING
JADAVPUR UNIVERSITY
KOLKATA- 7000032

SCHOOL OF NUCLEAR STUDIES & APPLICATION

FACULTY OF INTERDISCIPLINARY STUDIES, LAW AND MANAGEMENT

JADAVPUR UNIVERSITY

KOLKATA 700032

MAY 2019

JADAVPUR UNIVERSITY

FACULTY OF INTERDISCIPLINARY STUDIES, LAW AND MANAGEMENT

SCHOOL OF NUCLEAR STUDIES AND APPLICATION

CERTIFICATE OF RECOMMENDATION

This is to certify that the thesis entitled "**FAILURE ASSESMENT DIAGRAM ON LOW TEMPERATURE OF 20MnMoNi55 STEEL**", which is being submitted by **Anil Kumar Panja** in partial fulfilment of the requirements for the award of the degree of "**Master of Nuclear Engineering"** at the School of Nuclear Studies and Application, Jadavpur University, Kolkata700032, during the academic year 2017-2018, is the record of the student's own work carried out by him under our supervision.

Dr. Sanjib Kumar Acharyya
Thesis Adviser
Department of Mechanical Engineering
Jadavpur University, Kolkata 700032

Dr. Amitava Gupta
Director
School of Nuclear Studies and Application
Jadavpur University Kolkata 700032

Dean
Faculty of Interdisciplinary Studies,
Law and Management
Jadavpur University Kolkata700032

JADAVPUR UNIVERSITY

FACULTY OF INTERDISCIPLINARY STUDIES, LAW AND MANAGEMENT

SCHOOL OF NUCLEAR STUDIES AND APPLICATION

CERTIFICATE OF APPROVAL*

The foregoing thesis entitled "**FAILURE ASSESMENT DIAGRAM ON LOW TEMPERATURE OF 20MnMoNi55 STEEL**" is hereby approved as a creditable study of an engineering subject carried out and presented in a satisfactory manner to warrant its acceptance as a prerequisite for the degree of "**Master of Nuclear Engineering"** at the School of Nuclear Studies and Application, Jadavpur University, Kolkata700032, for which it has been submitted. It is understood that by this approval the undersigned do not necessarily endorse or approve any statement made, opinion expressed or conclusion drawn there in but approve the thesis only for the purpose for which it is submitted.

Committee on Final Examination
For Evaluation of the Thesis

Signature of Examiners

*Only in case the recommendation is concurred in

JADAVPUR UNIVERSITY

FACULTY OF INTERDISCIPLINARY STUDIES, LAW AND MANAGEMENT

SCHOOL OF NUCLEAR STUDIES AND APPLICATION

DECLARATION OF ORIGINALITY AND COMPLIANCE OF ACADEMIC ETHICS

It is hereby declared that the thesis entitled "**FAILURE ASSESMENT DIAGRAM ON LOW TEMPERATURE OF 20MnMoNi55 STEEL**" contains literature survey and original research work by the undersigned candidate, as part of his degree of "**Master of Nuclear Engineering"** at the School of Nuclear Studies and Application, Jadavpur University, Kolkata700032.

All information in this document has been obtained and presented in accordance with academic rules and ethical conduct.

It is also declared that all materials and results, not original to this work have been fully cited and referred throughout this thesis, according to rules of ethical conduct.

Name: **ANIL KUMAR PANJA**
Registration Number: **141079 OF 2017-18**
Examination Roll Number: **M4NUE19002**
Dated: **30.05.2019**

(Signature)
ANIL KUMAR PANJA
Master of Nuclear Engineering
School of Nuclear Studies and Application
Jadavpur University, Kolkata700032

ACKNOWLEDGEMENT

This project is by far the most significant accomplishment in my life and it would be impossible without people who supported me and believed in me.

Foremost, I would like to express my sincere gratitude to my guide ***Dr. Sanjib Kumar Acharyya*** *for the continuous support of my master degree study and Project, for his patience, motivation, enthusiasm, and immense knowledge. His guidance helped me in all the time of project and writing of this thesis. I could not have imagined having a better advisor and mentor for my master degree study.*

*I am very much thankful to my seniors and laboratory-in-charge of the '****Fatigue, Fracture and Damage Analysis Laboratory****' helped me a lot to understand and analysis the enormous testing data and also gave me substantial support in the software part.*

I also thank all of my friends who have more or less contributed to the preparation of this project .I will be always indebted to them.

Last but not least I would like to thank my parents, who taught me the value of hard work by their own example and give me the opportunity for education.

Anil Kumar Panja

Examination Roll No.: **M4NUE19002**

Registration No.: **141079 OF 2017-18**

ABSTRACT

Component or a structure may fail either due to fracture or plastic collapse or plastic deformation preceding fracture when it is subjected to loading. Understanding of the mode of failure of a particular component is thus very important from design point of view. To predict a component to be safe by performing a linear elastic fracture mechanics analysis is not enough because it gives no warning and at the same time cannot define the elastic-plastic interaction causing the failure of the component. Hence an analysis must be adopted that spans the entire range from linear elastic to fully plastic behaviour and one such analysis is Failure Assessment Diagram (FAD). FAD provides a means to determine the safety of a particular component under load. FAD also provides a theory of assessment of failure of a particular structural member based not only on fracture but also failure due to plastic collapse or contribution of both brittle fracture and plastic collapse on the structure or component taken into consideration. In this thesis an attempt has been made to study and development of different level of FAD for different geometry at different temperature based on CT specimen data and to verify the effect at lower temperature on different level of Failure assessment diagram. A comparison of different levels of FAD is shown along with the experimentally obtained results.

CONTENTS

List of figures:

List of Tables

NOMENCLATURE

K_r	Brittle Fracture Ratio
L_r	Plastic Collapse Ratio
Keff	Effective Stress Intensity Factor
K	Stress Intensity Factor
P	Applied Loa
P_0	Limit Load
σ_{ref}	Reference Stress
σ_{ys}	Yield Stress
σ_{flow}	Flow Stress
ε_{ref}	Reference Strain
E	Young's modulus
n	Poisson's Ratio
a	Crack Length
W	Width
B	Thickness
b	Un-cracked Ligament Length
FAD	Failure Assessment Diagram
γ	Gama
η	eta
RPV	Reactor Pressure vessel

Chapter 1: INTRODUCTION

The 20MnMoNi55 Steel is used in nuclear power plants for the production of nuclear reactor pressure vessels. It has 0.2 % carbon with 1.25% Mn , 0.5% Mo, 0.6% Ni with small quantity of Cr, Si and sulphur. From metallurgical point of view, increase of material strength may influence other properties such as toughness, corrosion resistance and may also affect the weldability. So good mechanical and metallurgical properties are required to withstand the internal pressure and prevent unexpected failure. This particular material 20MnMoNi55 steel has been the subject of extensive research work recently.

1.1 Nuclear Reactor

Most nuclear electricity is generated using reactors which were developed in the 1950s and improved since.

Generation I reactor (early prototypes, research reactors, non-commercial power producing reactors)

Generation II reactor (most current nuclear power plant 1965-1996)

Generation III reactor (evolutionary improvements of existing designs 1996-present)

Generation IV reactor (technologies still under development unknown start date, possibly 2030)

New designs are coming forward and some are in operation as the first generation reactors come to the end their operating lives. Over 16% of the world's electricity is produced from nuclear energy. A nuclear reactor produces and controls the release of energy from splitting the atoms of certain elements. In a nuclear power reactor, the energy released is used to make steam to generate electricity. In a research reactor the main purpose is to utilize the actual neutrons produced in the core. In most naval reactors, steam drives a turbine directly for propulsion. The principles for using nuclear power to produce electricity are the same for most types of reactor. The energy released from continuous fission of the atoms of the fuel is harnessed as heat in either a gas or water, and used to produce steam. This steam is used to drive the turbines which produce electricity.

1.2 Reactor Pressure Vessel

The RPV is cylindrical with a hemispherical bottom head and a flanged and gasket upper head. The bottom head is welded to the cylindrical shell while the top head is bolted to the cylindrical shell via the flanges. The cylindrical shell course may or may not utilize longitudinal weld seams in addition to the girth (circumferential) weld seams. The body of the vessel is of low-alloy carbon steel. To minimize corrosion, the inside surfaces in contact with the coolant are covered with a minimum of some 3 to 10 mm of austenitic stainless steel. Numerous inlet and outlet nozzles, as well as control rod drive tubes and instrumentation and safety injection nozzles penetrate the cylindrical shell. The number of inlet and outlet nozzles is a function of the number of loops or steam generators.

Reactor pressure vessels contains nuclear fuel core. So, the integrity of the RPV material must be guaranteed. The RPV must resist brittle fracture under all operational and environmental condition. Improvement of RPV design required advance fracture mechanics concept and analysis is required. To justify the integrity of RPV material required the fracture toughness of the material. A high value of fracture toughness indicates that material undergoing ductile fracture while lower value indicates brittle fracture.

1.3 Fracture Toughness

In real world no material is flawless and consists of very small cracks. This crack is caused by discontinuities in assembly, harsh environmental condition and material defects. Flaws are not avoidable in the material. A lot of research has been carried out in the recent past to characterise the behaviour of the material consisting of crack. There are different fracture parameters which have been developed to characterise the behaviour of material subjected to different modes of loading. The different fracture parameters are $K_{IC,}$ CTOD, J_{IC} etc. These parameters predict the state of stress at the crack front and the resistance of a material to failure. The stress at the tip of a crack is defined with the help of stress intensity factor. For a brittle material when the value of stress intensity factor becomes greater than the surface energy between the bonds then the corresponding stress intensity factor is reffered to as $K_{IC.}$ For ductile materials the stress at the crack tip cannot be defined with the help of stress intensity factor and hence a new fracture parameter was developed known as J-integral. For

a ductile material consisting of cracks the sequence for failure is crack initiation followed by stable crack growth finally leading to instability. The crack initiation point for a ductile material is well characterised in terms of J_{Ic} while the stable crack growth phenomenon can be characterised with the help of J versus Δa curve. The estimation of J_{IC} from J versus Δa curve is described in details in chapter 3 and chapter 4 respectively.

1.4 Fundamental Ideas of Fracture mechanics

Fracture mechanics is the study of mechanics with the crack propagation in material. Fracture mechanics is also applied to crack growth under fatigue loading. Initially, the fluctuating load nucleates a crack, which then grows slowly and finally the crack growth rate per cycle picks up speed. Thereafter comes in a stage when the crack-length is long enough to be considered critical for a catastrophic fracture failure.

This now enables a designer to use a much lower factor of safety. A parameter to measure crack potency is required when geometry of a crack in a structural component, loads and other boundary conditions are known.

1.5 Fracture Parameters

The analysis of fracture mechanics problem is done through different approaches, each one having its own parameter –

- **Energy Release Rate (G) -** is energy based and is applied to brittle or less ductile materials.

- **Stress Intensity Factor (K) -** is stress based, also developed for brittle or less ductile materials.

- **J-Integral (J) -** has been developed to deal with ductile materials. Its formulation is quite general and can be applied to brittle materials also.

- **Crack Tip Opening Displacement (CTOD**) - parameter has been also developed for ductile materials.

1.6 Failure Assessment Diagram

A truly homogenous defect-free structure is impossible to achieve. The acceptance that defects will be present in structures makes the study of how they affect structural integrity an important subject.

There are two different types of failure: Brittle failure and Failure by plastic collapse. If a plate with a crack is considered and let axial loading be applied on it. When the components separate into two different parts, without any prior warning it is said to be brittle failure. However, If the material undergoes plastic deformation before leading to final instability then the failure is referred to as ductile failure.

Hence it is necessary to asses both the conditions for failure. It has to be examined regarding the mode of failure that has taken place for a material subjected to loading. Thus, the concept of FAD was introduced to understand the mode of failure for a particular component or specimen.

The Failure Assessment Diagram (FAD) is probably the most widely used methodology for elastic-plastic fracture mechanics analysis of structural components. The FAD approach was originally introduced in 1975 by Dowling and townley [2]. The first procedure of FAD using two criteria approach is purely based on strip yield model by Harrison et al [3]. It was based on two parameter brittle fracture ratio Kr and Load ratio Sr.

Where,

$$K_r = \frac{K_I}{K_{eff}} \tag{1.1}$$

$$S_r = \frac{\sigma}{\sigma_c} \tag{1.2}$$

$$K_I = \sigma\sqrt{\pi a} \tag{1.3}$$

$\mathrm{K_{eff}}$ = Effective stress intensity factor

The Effective stress intensity factor through a crack in an infinite plate, according to strip yield model is given below:

$$K_{eff} = \sigma_{ys}\sqrt{\pi a}\left[\frac{8}{\pi^2}\ln\sec\left(\frac{\pi\sigma}{2\sigma_{ys}}\right)\right]^{\frac{1}{2}} \quad (1.4)$$

Equation 1.4 , can be modified for real structure by replacing σ_{ys} with σ_c for the structure. This would ensure that the strip yield model predict failure on the applied stress approaches to the collapse stress. The next step in deriving a failure assessment diagram from the strip-yield model entails dividing the effective stress intensity by the linear elastic *K*.

$$\frac{K_{eff}}{K_I} = \frac{\sigma_c}{\sigma}\left[\frac{8}{\pi^2}\ln\sec\left(\frac{\pi\sigma}{2\sigma_c}\right)\right]^{\frac{1}{2}} \quad (1.5)$$

Thus Equation 1.5, removes the geometry dependence of the strip-yield model. The failure assessment diagram is then obtained by inserting the above definitions into Equation 1.5 and taking the reciprocal for the assessment curve which is given below:

$$K_r = S_r\left[\frac{8}{\pi^2}\ln\sec\left(\frac{\pi}{2}S_r\right)\right]^{\frac{1}{2}} \quad (1.6)$$

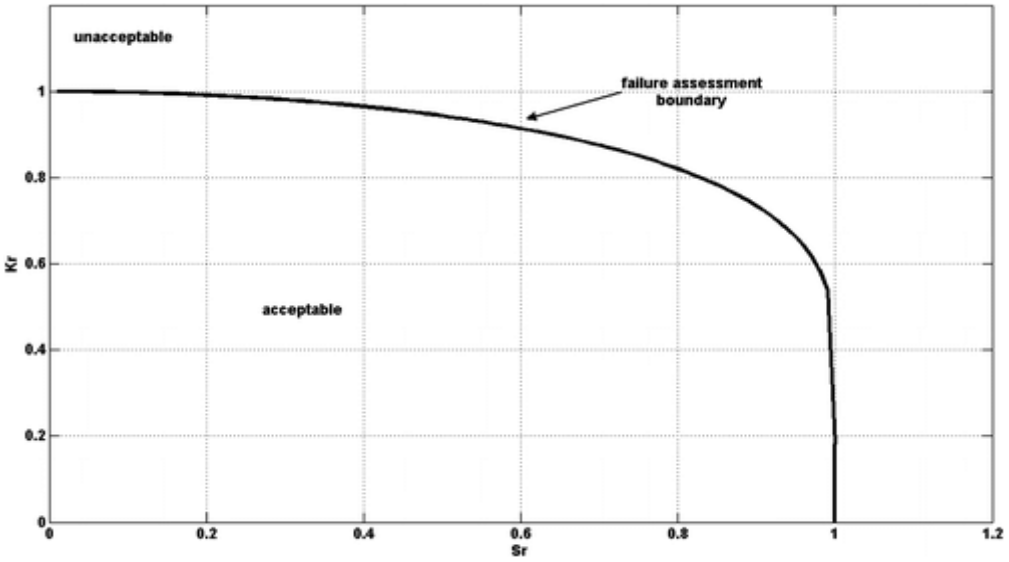

Fig1.1: The strip yield failure assessment diagram

The curve represents the locus of predicted failure points. If the toughness is very large, the structure fails by collapse when S_r = 1.0. A brittle material will fail when K_r = 1.0. In intermediate cases, collapse and fracture interact, and both K_r and S_r are less than 1.0 at failure. All points inside of the FAD are considered as safe, points outside of the diagram are

unsafe. Hence the locus of failure point obtained according to equation 1.6 considers the effect of both fracture and plastic deformation. But this concept of failure assessment diagram from the strip yield model is no longer in use as it does not account for strain hardening. To consider the strain hardening in the Failure Assessment Diagram, the definition of Kr and Sr was no more applicable when there is strain hardening.

In order to assess the significance of a particular flaw in a structure, one must determine the toughness ratio as follows:

$$K_r = \frac{K_I}{K_{mat}} \tag{1.7}$$

$$L_r = \frac{P}{P_0} = \frac{\sigma_{ref}}{\sigma_{ys}} \tag{1.8}$$

Where,

$K_I = Stress\ intensity\ factor$

$K_{mat} = Fracture\ toughness\ of\ the\ material$

P = Load

$P_0 = Limit\ Load$

$\sigma_{ref} = Reference\ stress$

$\sigma_{ys} = Yield\ stress$

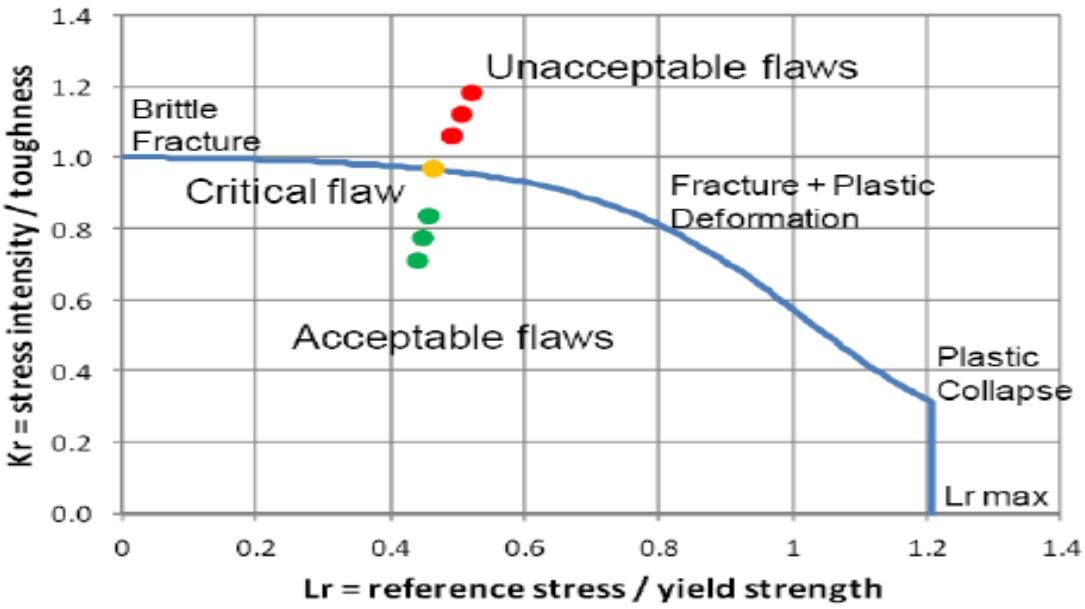

Fig 1.2: Failure assessment diagram (FAD), which spans the range of fully brittle to fully ductile behaviour.

Generally, K_r = 1 represents the brittle fracture and L_r = 1.2 represents the Plastic collapse conditions which is basically the two particular points of the curve represent when the following conditions satisfy:

(K_r =1, L_r =0) = Brittle fracture

(K_r =0, L_r =1.2) = Plastic collapse

If the assessment point falls inside the FAD, the structure is considered safe. Failure is predicted when the point falls outside of the FAD. The nature of the failure is a function of where the point falls. When both the toughness and applied stress are low (small L_r and large K_r), the failure occurs in the linear elastic range and usually is brittle. At the other extreme (large L_r and small K_r), the failure mechanism is Plastic collapse.

In 1976, the Central Electricity Generating Board in the UK published the first procedure of FAD using Two Criteria Approach. Since the first publication, various changes have been implemented and the current procedure is called R6 procedure [3], which is revised further.

Bloom [4] and Shih et al [6] showed that a *J*-integral solution from the EPRI handbook could be plotted in terms of a FAD. Of course, a more rigorous *J* solution based on elastic-plastic finite element analysis can also be plotted as a FAD. The failure assessment diagram is nothing more than an alternative method for plotting the fracture driving force. The shape of the FAD curve is a function of plasticity effects. A *J* solution merely provides a more accurate description of the FAD curve.

The most rigorous method to determine a FAD curve for a particular application is to perform an elastic-plastic *J* integral analysis. Such an analysis can be complicated and time consuming, however. Simplified approximations of the FAD curve are given below:

Level 3A FAD,

When stress-strain data are not available for the material of interest, the following FAD expressions may be used to developed the FAD curve,

$$K_r = [1 - 0.14(L_r)^2]\{0.3 + 0.7exp[-0.65(L_r{}^6)]\} \quad (1.9)$$

Where,

$$K_r = f(L_r) \quad (1.10)$$

$$L_r = \frac{P}{P_0} \quad (1.11)$$

P = Load

P_0 = Limit Load

$$P_0 = 1.455\eta B b_0 \sigma_{flow} \quad \text{(Plain strain)} \tag{1.12}$$

Where,

η = Dimensionless constant.

B = Thickness of Compact Tension Specimen.

b_0 = Initial Un-cracked ligament length.

σ_{flow} = Flow stress = $\frac{(\text{Yield stress} + \text{Ultimate stress})}{2}$

$$\eta = \sqrt{(\frac{2a}{b})^2 + \frac{4a}{2} + 2} - (\frac{2a}{b} + 1) \tag{1.13}$$

a= Initial Crack Length

b = Initial Un-cracked ligament length

Load and Limit load can be obtained from the experimental fracture test results of CT specimen. The Limit Load is calculated in terms of the η-factor and Flow stress. Here the flow stress is the average value of the yield stress and ultimate stress which is given in the experimental result.

The empirical relationship of level 3A FAD cannot consider strain hardening. So, it is a material independent and geometry independent FAD curve.

Level 3B FAD,

It is based on the reference stress approach, accounts for the material dependence in the FAD curve but assumes that it is geometry independent. The FAD curve reflects the shape of the stress-strain curve. Therefore, Equation 1.14 predicts a FAD that is unique for each material. The expressions for FAD:

$$K_r = \left[\left(1 - \alpha {L_r}^{n-1}\right) + \frac{1}{2} \frac{{L_r}^2}{1 + \alpha {L_r}^{n-1}} \right]^{-\frac{1}{2}} \tag{1.14}$$

When the stress-strain data are available for the material, then ϵ_{ref} and σ_{ref} data are used for the construction of empirical relationship. The reference strain is inferred from the true stress-true strain curve at various reference stress value.

$$L_r = \frac{\sigma_{ref}}{\sigma_{ys}} \tag{1.15}$$

So, the above equation can be modified as shown in equation 1.16,

$$K_r = [\left(1 + \alpha {L_r}^{n-1}\right) + \frac{{L_r}^2}{\left(1 + \alpha {L_r}^{n-1}\right)}]^{-1/2} \tag{1.16}$$

According to the Ramberg-Osgood power law relationship,

$$\frac{\varepsilon_{ref}}{\varepsilon_{ys}} = \frac{\sigma_{ref}}{\sigma_{ys}} + \alpha \left(\frac{\sigma_{ref}}{\sigma_{ys}}\right)^n \tag{1.17}$$

Where, α and n are the material properties also known as Ramberg-Osgood parameter.

The experimental stress-strain data can be used to calculate Ramberg-Osgood parameter and the expressions are given below,

Ramberg-Osgood equation can be re-written as-

$$\varepsilon_p = \alpha \frac{\sigma}{E} \left(\frac{\sigma}{\sigma_0}\right)^{n-1} \tag{1.18}$$

It can be observed from level 3B FAD that it is depend on material property where α and n determines the nature of the curve and as the values of n decreases there is a more gradual tail in the FAD curve. Therefore the equation 1.16 predicts a FAD curve that unique for each material.

Level 3C FAD,

Finite element simulations are carried out for the each and every model individually. So, both the properties of the material are taken into consideration. Therefore, level 3C FAD is obtained from the elastic-plastic finite element analysis result to consider material properties and geometry properties.

Different CT specimen with different a/w ratio at different temperature conditions are required to simulate. Kr and Lr values are calculated from the Finite element simulation results which is used to construct the level 3C FAD.

$$K_r = \sqrt{\frac{J_{el}}{J_{total}}} = \frac{K_I}{K_J} \quad (1.19)$$

$$L_r = \frac{P}{P_0} = \frac{\sigma_{ref}}{\sigma_{ys}} \quad (1.20)$$

Where,

J_{el} = Elastic J-integral

J_{total} = Total J-integral

σ_{ref} = Reference stress

σ_{ys} = Yield stress

P = Load

P_0 = Limit Load

Here, the load and limit load calculation is same as described in the level 3A FAD but the values of load must be obtained from the finite element simulation results. The experimental stress-strain data required to simulate elastic-plastic modelling. The J-integral values are calculated from the finite element simulation result which is described in the finite element chapter and the values are required because it is a function of K_r .

It can be observed from the level 3C FAD curve that both the material properties and geometry of the component is consider in level 3C FAD. Level 3C FAD curve changes its locus depends on the material property and geometry.

1.7 Significance of different levels of FAD

Level 3A FAD is used for assessment of failure curve when the stress strain data are not available, finite element simulation tools are not available and there is no scope to geometry analysis. It is the universal curve for every material and it cannot specify some specific features. So, a material and geometry specific FAD curve is needed.

Whenever the stress-strain data of the material are available then Level 3B FAD is used for the assessment of failure curve. Level 3B FAD expression includes strain hardening which is not used in the level 3A FAD expression. Level 3B FAD considered material property as the stress-strain data are used for the construction of level 3B FAD. Finite element simulation tools are not used to develop the level 3B FAD, so it does not consider geometry factor in it because geometry correction is not included in it. Whenever the material stress-strain data

are available then it's better to apply level 3B FAD than level 3A FAD because it can take care of the hardening effect.

Level 3C FAD can be used only when the Stress-Strain data and finite element simulation tools are available. Geometry and material dependent FAD curve is required to consider the material property and geometry factor in it. Material property and geometry factor are used to construct level 3C FAD. So, whenever a material and geometry dependent FAD is required the level 3C FAD gives the best fit.

1.8 Objective of the thesis:

The Failure Assessment Diagram has been widely accepted for assessing and the integrity of cracked and damaged material structure. It is a graphical representation of two non-dimensional parameter failure criteria which are Brittle fracture and Plastic collapse. It is also provides the assessment of failure for both the brittle fracture and plastic collapse on the material.

The objective of this thesis is to study and development of different level of FAD for different geometry at different temperature based on CT specimen data and to verify the effect at lower temperature on different level of Failure assessment diagram.

Steps to achieve the objective:

I. Experiments were carried out for Tensile and CT specimens at different temperature. Experiment provides the important data which was used for the construction of FAD and Finite Element Simulation.
II. Finite element simulations were carried out for stationary crack growth of CT specimen at different temperature.
III. Construction of level 3A FAD curve for different temperature and a/W with the help of empirical relationship.
IV. Construction of level 3B FAD curve for different temperature and a/W with the help of the empirical relationship and compared with the level 3A FAD.
V. Construction of level 3C FAD curve for different temperature and a/W with the help of Finite Element Simulation for stationary crack growth at different temperature.
VI. Temperature effect on level 3C FAD at different temperature which is also effects on the contribution of brittle factor.

1.9 Summary of the Thesis:

This thesis is mainly based on seven chapters and each of chapter is used to describe the objective of the thesis.

I. Introduction is the first chapter which includes the history prospects of Failure Assessment Diagram, general introduction of Fracture Mechanics, idea of Failure Assessment Diagram and the brief description of the objective of this thesis.

II. The second chapter is all about the Literature Review. Different type of research on Failure Assessment diagram and required experimental work up to the present time are studied, surveyed and described in short notes for the solution of the present work.

III. Material and Test procedure details is the third chapter which includes different type of test and experiments of different specimen required for this work at different temperature with the collection of data from the experiments for the further analysis.

IV. Finite Element Simulation is the fourth chapter and it described the information of simulation carried out for the specimen. Stationary crack growth of CT specimen was simulated and the collection of result was described in this chapter.

V. Fifth chapter named as Development of different Levels of FAD provides Different level of Failure Assessment Diagram for different temperature and a/W. The details study of construction of level 3C FAD at different temperature from the finite element simulation results. It also described that how the FAD changed depend on temperature variation.

VI. Sixth chapter is about the general conclusion and it described that the thesis has achieved its objectives.

Chapter 2: LITERATURE REVIEW

The first FAD approach was originally introduced in 1975 by Dowling and townley [2]. The first procedure of FAD using two criteria approach is purely based on strip yield model by Harrison et al [3]. It was based on two parameter brittle fracture ratio Kr and Load ratio Sr but it has some limitation that it does not consider strain hardening.

In 1976, the Central Electricity Generating Board in UK incorporated the strip yield failure assessment into a fracture analysis methodology, which is known as the R6 approach [3]. Since the first publication, enormous changes have been done, which was revised in 1980, 2001, 2009.

In the year 1980, Bloom [4] and shih et al [6] showed that a J-integral solution from the ERPI handbook could be plotted in terms of FAD. A more rigorous J solution based on elastic plastic finite element analysis can also be plotted.

PD6493:1980 concentrated on the assessment of imperfections with regard to their possible effects on failure by brittle fracture and fatigue. The treatment for brittle fracture was based on measurements of fracture toughness in terms of K_{Ic} or CTOD (crack tip opening displacement) and utilised the CTOD design curve proposed by Burdekin and Dawes [1].

J-estimation procedures based on finite-element solutions are expressed in terms of the material stress-strain curve by Ainsworth, R.A [7]. in the year 1984, using reference stress technique. The result is an exact representation of the estimation procedures for materials which strain harden according to the simple power law used in the finite-element calculations. The resulting reference stress based estimation procedure is used to derive a failure assessment curve for use with the CEGB failure assessment route. Comparison is made with the modified failure assessment curve recently suggested by Milne.

In the year 1984, A failure assessment diagram is derived by R.BRADFORD, R.S. GATES, G GREEN and D.C WILLIAMS [8] from carbon-manganese steel CT specimen. The diagram has

been determined from an elastic-plastic finite element analysis of a CT specimen geometry. The diagram has been validated by using experimental fracture toughness data obtained on the same material and geometry modelled in the finite element analysis. It is shown that a non-work-hardening failure assessment diagram is not a good representation of the experimental data and that the computed failure assessment diagram is more appropriate for describing the behaviour of the carbon-manganese steel specimens.

It is concluded by Milne, I., Ainsworth, R.A., Dowling, A.R., Stewart, A.T [9] that the procedures presented in the third revision of R6 are valid. The use of moderately pessimistic input data in assessments will ensure that failures are avoided. The third revision of the CEGB procedures for the 'Assessment of the Integrity of Structures Containing Defects', R6, provides background information and validation. The background information includes details of the derivation, demonstrating the strong theoretical foundation of the procedures. Validation is addressed by comparison with tests on simple specimen geometries and structural components. This is supported and extended by comparing the procedures with the results of finite-element analyses.

In PD6493:1980 [5], there were two such method available was a possible source of confusion. So, PD6493:1980 [5] was reissued in 1991 and it describe that the treatment of fatigue remained very similar to that in the 1980 edition but for the treatment of ductile and brittle fracture was changed in PD6493:1991 [11] and three level of assessment were given :
Level 1, termed the 'Preliminary Assessment' method, was similar to that in the 1980 edition, except that a failure analysis diagram was used, so that the treatment for plastic collapse was considered.
Level 2, the 'Normal Assessment' method was similar to that of the revision 2 of R6 method.
Level 3, termed the 'Advanced Assessment' method was based on revision 3 of R6 and allowed the user to take account of the resistance to ductile crack extension. Other changes in the 1991 edition were that the treatments from some of the other failure modes were enhanced.
Crack growth initiation and subsequent resistance is computed by VIGGO TVERGAARD and JOHN W. HUTCHINSON [12] for an elastic-plastic solid. Three applications of the results are made,

1. To predict toughness when the fracture process is void growth and coalescence,
2. To predict the role of plasticity on interface toughness for similar materials bonded together,
3. To illuminate the role of plasticity in enhancing toughness in dual-phase solids.

The regime of applicability of the present model to ductile fracture due to void growth and coalescence, wherein multiple voids interact within the fracture process zone, is complementary to the regime of applicability of models describing the interaction between a single void and the crack tip. The two mechanism regimes are delineated and the consequence of a transition between them is discussed.

PD 6493 [11] (Guidance on methods for assessing the acceptability of flaws in fusion welded structures), has now been revised again and published as BS7970:1999 "Guidance on Methods for Assessing Acceptability of Flaws in Metallic Structures" [13]. It includes a number of new structural integrity tools, and industry-specific application guides and it incorporates additional structural and defect geometries.

A failure assessment diagram (FAD) curve is employed to graphically characterize the effect of plasticity' on the crack driving force by EDWARD FRIEDMAN and WILLIAM K.WILSON [14]. The Option 1 FAD curve of the Level 3 advanced fracture assessment procedure of British Standard PD 6493:1991 [11], adjusted for stress concentration effects by a term that is a function of the applied load and the ratio of the local radius of curvature at the flaw location to the flaw depth, provides a satisfactory bound to all the FAD curves derived from the explicit flaw finite element calculations.

Stress-based fracture assessment procedure introduced by P.J.BUDDEN [15] , which contain conservatism when assessing strain- or displacement-controlled loads in excess of yield and an alternative strain-based methods are discussed and compared with an existing approach in the R6 defect assessment procedure that allows reduction in conservatism for the case of fixed displacement or rotation loading. Finite element results for semi-elliptical cracks in plates are re-interpreted as values of J against remote strain and used to assess recent strain-based estimates of J.

To evaluate if a crack may cause structural failure, the failure assessment diagram (FAD) uses two ratios: brittle fracture and plastic collapse. C. Tipple, and G. Thorwald [16], described that Abaqus is used to compute elastic-plastic J-integral results along the crack front. These results are then used to calculate the plastic collapse crack reference stress, especially for cases when the reference stress solution is not available for a structural component.

Marcos A.Bergant et al [17] 2013 proposed an alternative more realistic methodology based on the Failure Assessment Diagram. This FAD was used for predicting the failure modes (ductile fracture or plastic collapse) of defective SGTs for varied crack geometries and loading conditions. The present analysis indicates the potentiality of the FAD as a comprehensive methodology for predicting the failure loads and failure modes of flawed SGTs. Experimental determination of fracture toughness of SGT materials were firstly reviewed for this methodology.

Ultra-high-strength steels are sensitive to heat input during welding, which can lead to softening in the heat-affected zone. This softening can also reduce the limit load capacity in non-load-carrying welds. It is important to address this phenomenon in the design phase. Ilkka Valkonen [18] 2014 introduce a procedure using notched specimens to determine material parameters and failure criteria and results show that the developed method results agree with results from the component test.

Sang-hyun kim et al [19] 2016 introduce a simplified limit load estimation for branch pipe junctions under internal pressure and in-plane bending which is m_σ-tangent method. This method is based on a linear elastic finite element analysis to estimate the limit loads, but it does not guarantee accurate limit load estimation. Nevertheless, m tangent method is rapid method to obtain limit load for complex geometry and loading conditions for specific cases.

Chapter 3: MATERIAL AND TEST PROCEDURE DETAILS

3.1 Introduction

The 20MnMoNi55 Steel of current interest is used in nuclear power plants for the production of nuclear reactor pressure vessels. So, 20MnMoNi55 Steel is used for our investigation and the material was received from Bhabha Atomic Research Centre, Mumbai, India. Rectangular block shaped material (20MnMoNi55 Steel) was received from the above institution. Tensile specimens and CT specimens were made from the material to determine the fracture toughness of the material.

The chemical composition of the material is given below –

Name of Element	C	Si	Mn	P	S	Al	Mi	No	Cr	Nb
Percentage Composition (in weight)	.20	.24	1.38	0.011	0.005	0.068	0.52	0.30	0.06	0.032

Table 1- Chemical Composition of Material (20MnMoNi55)

Experiments of CT and Tensile specimens were carried out at different temperature and different geometry for the determination of fracture toughness for this material (20MnMoNi55). The data collected from those experiments were used to construction of different level of FAD and for the Finite Element Simulation.

To develop different level of FAD at different temperature, tensile specimen test and fracture test is required. Tensile test gives the experimental stress-strain data which is required to develop level 3B FAD whereas level 3C FAD requires finite element simulation results. So, the experimental test and finite element simulation are required to achieve the objective of this thesis.

3.2.1 Tensile Testing

A tensile test, also known as a tension test, is one of the most fundamental and common types of mechanical testing. A tensile test applies tensile (pulling) force to a material and measures the specimen's response to the stress. By doing this, tensile tests determine how strong a material is and how much it can elongate. Tensile tests are typically conducted on Universal Testing Instruments. In this analyses the tensile tests were done at 22°C, 0°C, -40°C,-80°C,-100°C.All the collected data from the tests were used to determine the stress-strain data and material properties. Properties that are directly measured from the test are Ultimate tensile strength, breaking strength, maximum elongation. From these measurements the following material properties can be determined: Young modulus, Poison's ratio, Yield strength and material hardening characteristics. These are the data which is used as input to determine the fracture toughness and J-integral values for the material.

Fig 3.1: Arrangement of Universal Testing Machine (INSTRON8801)

3.2.2 Tensile Test Specimen

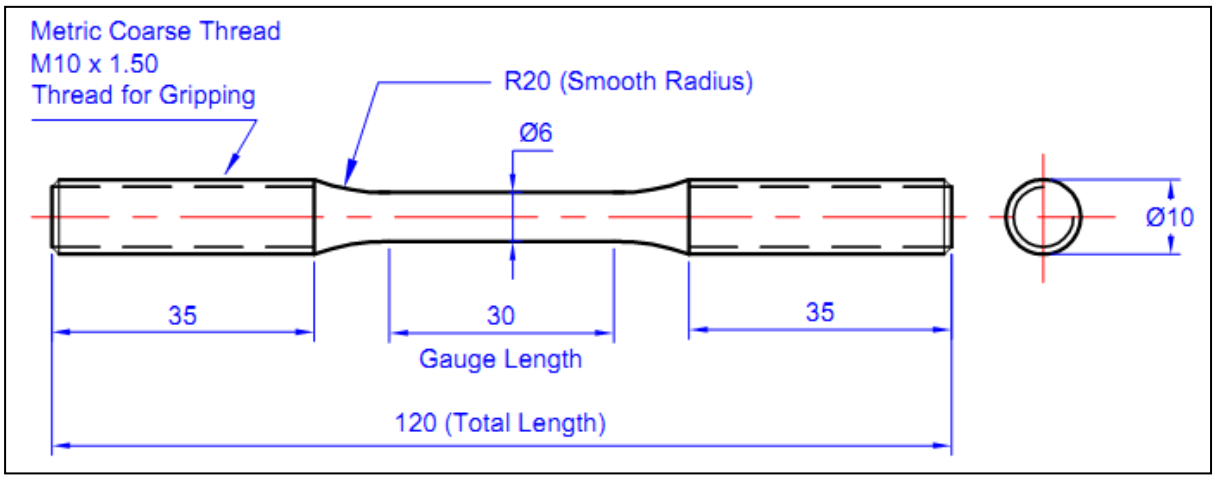

Fig 3.2: Schematic Diagram of tensile Specimen

3.2.3 Tensile Test Procedure

All tensile tests were done in a computer controlled Universal Testing Machine (INSTRON8801) attached with Cryo-chamber (Model No.-3119-408, Serial No.-0005120) with the capacity of 100KN grid. Threaded end of the specimen were attached with the load cell and actuator through pin which was loaded by adapter.

Flowing Liquid Nitrogen was used to maintain the different test temperatures which is supplied from a fully automated self- pressurizing Dewar Flask of 120 Litres capacity supplied by M/S Instron, UK. A type K thermocouple via the eurotherm 2408 controller was used for control over the chamber temperature eurotherm 2408 controller drives the heater through a solid state relay (SSR) and also the coolant solenoid valve.

The power to the chamber was switched ON which is controlled by the contact breaker switch on the rear panel of the chamber .The chamber was securely mounted in the test position and its door was required to kept closed. The required set point temperature was maintained by the two buttons UP and DOWN. The fan was used for the thermal control as well as cooling.

Minimum 30 minutes is required for maintaining of equilibrium temperature of the chamber so that test temperature was achieved uniformly in the whole portion of the specimen. Then required software was used for loading condition of the specimen

The experimental Stress-Strain curves at different temperature are given below:

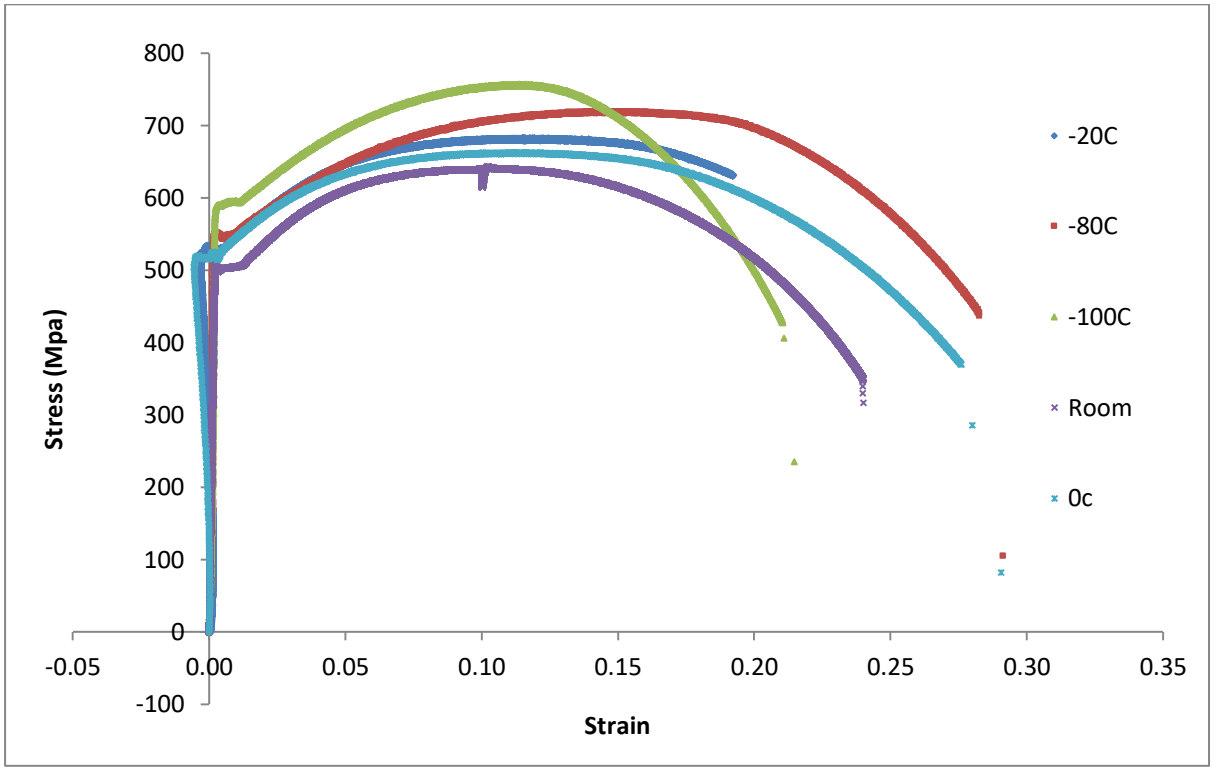

Fig 3.3: Experimental Stress-Strain curve of Tensile Specimen at different temperature

It can be observed from the above figure 3.3 that expected general phenomenon of embrittlement is not reflected in the stress strain curve as the temperature decrease. Lowering the temperature it is expected that fracture strain will decrease as material loses ductility which is not found for this material. However the effect of notch is not considered in this tensile test and it is to be seen if the presence of notch will affect the behaviour of material at sub-zero temperatures.

3.3.1 Fracture Test

Fracture toughness tests measure a material's ability to resist the growth or propagation of a pre-existing flaw. The flaw or defect may be in the form of a fatigue crack, void, or any other inconsistency in the test material. Fracture toughness tests are performed by machining a test sample with a pre-existing crack and then cyclically applying a load to the side of the crack so that it experiences forces that cause it to grow.

3.3.2 Fracture Test Specimen

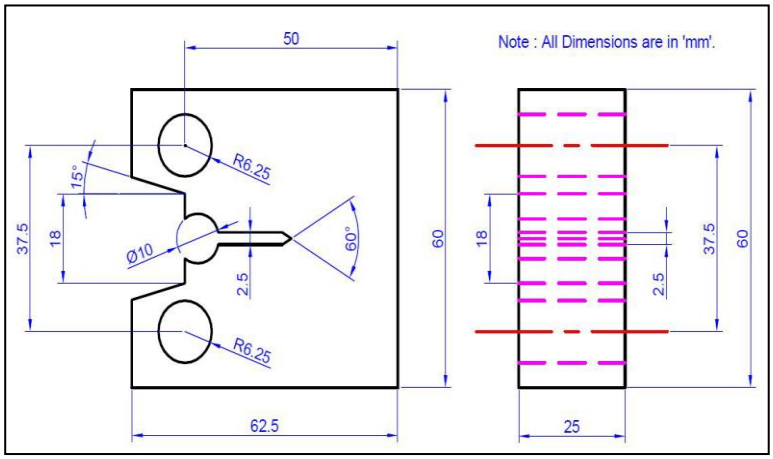

Fig 3.4: Schematic Diagram of CT Specimen

3.3.3 Fracture Test Procedure

The INSTRON UTM (Universal Testing Machine) with 8810 controller with 100 KN grid capacity is used for the estimation of J-integral values of the specimens as described earlier. The tests were done at different temperatures ranging from 22°C to -100°C.

According to the ASTM Standard test method E813 [23] , Fracture Toughness test on metallic materials performs. The J-integral values were determined by the INSTRON FAST TRACK JIC Fracture Toughness Program. The method is applied specifically to specimens that have notches or flaws that are sharpened with fatigue cracks. The loading rate was slow, and cracking caused by environmental factors was considered negligible. The JIC program determine crack growth by various way like unloading compliance, but other methods, such as DC Potential Drop (DCPD), can also be used. This analysis used the single specimen unloading compliance technique for evaluation of J-integral fracture toughness. In this method the crack lengths were determined from elastic unloading compliance measurements. This was done by carrying out a series of sequential unloading and reloading during the test.

3.3.4 Fatigue Pre-Cracking

The definition of fatigue testing is as simply applying cyclic loading to your test specimen. The load application can either be a repeated application of a fixed load or simulation of in-service loads. A servo-hydraulic fatigue testing machine is usually used to perform a fatigue

test. The test system should be fitted with a control system that is capable of controlling the test and measuring data

3.3.5 Fatigue Pre-Cracking Test Procedure

In this analysis investigation of the fatigue pre-cracking tests were carried out on Compact Tension specimens. According to the guidelines of ASTM E 1820 [21] Standard 1T CT specimens were machined. The designed dimensions of the compact tension specimen were thickness (B) =25 mm and width (W) = 50mm which was constant for all the specimen and machined different a/W ratio of 0.45, 0.47, 0.49, 0.55. According to the ASTM standard E 647 [22] at constant ΔK mode, Fatigue pre-cracking of the CT specimens was carried out at room temperature on servo hydraulic INSTRON UTM (Universal Testing Machine) with 8800 controller having 100 KN grid capacity using a commercial da/dN fatigue crack propagating software supplied by INSTRON Ltd U.K.. A COD gauge length was used for the crack length measurement which was mounted on the load line of the specimen by compliance technique. The gauge was connected to STRAIN 1 connector. The software permitted on-line monitoring of the crack length (a), stress intensity factor (ΔK) and the crack growth rate per cycle, da/dN. All pre-cracking experiments were carried out at a stress ratio of R = 0.1 using an initial frequency of 10 Hz and with a constant, (ΔK) = 30MPa√m.

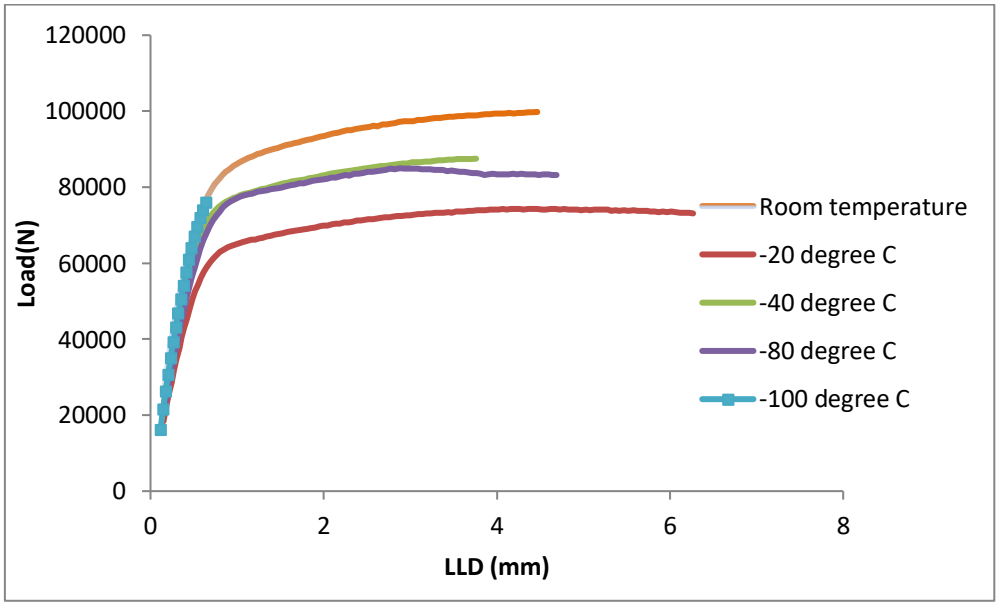

Fig 3.5: Experimental Load-Displacement curve of CT specimen at different temperature

Serial No.	Specimen Type	Type Of Test	Temperature (˚C)	Gauge Length (mm)	a/w Ratio	Thickness (mm)	No. of Test
1.	Tensile Round Specimen	Tensile Test	22	30.00	N/A	N/A	1
			-20	31.71			1
			-40	30.15			1
			-80	28.25			1
			-100	29.88			1
2.	Compact Tension Specimen	Fracture Test	22		0.45	25	1
					0.47		1
					0.49		1
					0.55		1
			-20		0.54		1
			-40		0.49		1
			-80		0.53		1
			-100		0.50		1

Table 2 – List of Experiments Carried Out

3.4 Calculation of J-Integral from experimental data

The calculation of J-integral from the load-displacement data according to the procedure described in ASTM E 1820 [21],

The J-integral is given by:

$$J_{total} = J_{el} + J_{pl} \tag{3.1}$$

Where,

The elastic J is computed from the elastic stress intensity:

$$J_{el(i)} = \frac{{K_{(i)}}^2(1 - v^2)}{E} \tag{3.2}$$

Where,

K = Instantaneous stress intensity factor which is related to the current values of load and crack length.

$$K_I = \frac{P}{B\sqrt{W}} f\left(\frac{a}{W}\right) \tag{3.3}$$

Where,

P – Applied load

B – Thickness of the specimen

W – Width of the specimen

f(a/W) – Dimensionless geometry function for a compact tension specimen

where,

f(a/W) for a compact tension specimen is given below,

$$f\left(\frac{a}{W}\right) = \frac{2 + \left(\frac{a}{W}\right)}{(1 - (a/W))^{\left(\frac{3}{2}\right)}}\left[0.886 + 4.64\left(\frac{a}{W}\right) - 13.32\left(\frac{a}{W}\right)^2 + 14.72\left(\frac{a}{W}\right)^3 - 5.60\left(\frac{a}{W}\right)^4\right] \tag{2.4}$$

The basic procedure in ASTM E 1820 [21] includes a simplified method for computing J_{pl} from the plastic area under the load-displacement curve,

$$J_{pl(i)} = \left[J_{pl(i-1)} + \left(\frac{\eta_{(i-1)}}{Bb_{(i-1)}}\right)\frac{(P_i + P_{(i-1)})(\Delta_{i(pl)} - \Delta_{i-1(pl)})}{2}\right] * \left[1 - \gamma_{i-1}\left(\frac{a_i - a_{i-1})}{b_{i-1}}\right)\right] \quad (3.5)$$

Where,

$J_{pl(i)}$– Plastic J computed from the area under load-displacement curve at each time increment.

P_i– Load at each time increment.

$\Delta i(pl)$–Plastic displacement at each time increment.

B – Net thickness of the specimen

$b_{(i)}$– Un-cracked ligament length at a given time increment.

H – Dimensionless constant.

a_i– Crack length at each time increment.

γ- Dimensionless constant.

Where,

$$\eta = 2 + 0.522\left(\frac{b_i}{W}\right) \quad (3.6)$$

$$\gamma_i = 1 + 0.76\left(\frac{b_i}{W}\right) \quad (3.7)$$

Calculated J-integral and crack extension of the specimen are plotted below and this curve is known as J-R curve,

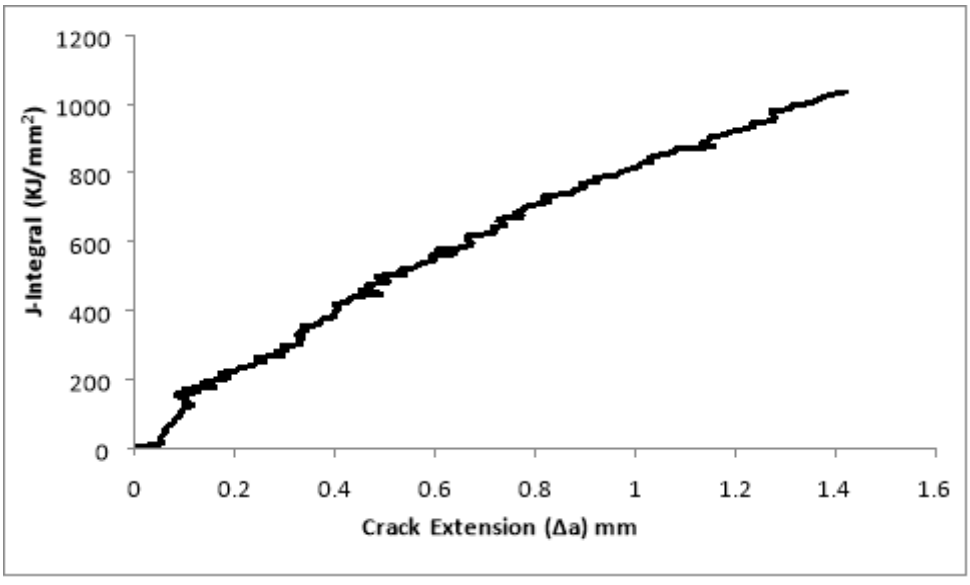

Fig 3.6: Experimental J-R curve

J_{IC} is determine from the J-R curve according to the procedure describe in the ASTM E 1820 [21]. It described that drawn a construction line accordance with the following equation,

$$J = 2\sigma_y \Delta a \quad (3.8)$$

Where,

J= J integral

Δa= Crack Extension

Plot the construction line, draw an exclusion line parallel to the construction line intersecting the abscissa at 0.15 mm. Draw a second line parallel to the construction line intersecting the abscissa at 1.5 mm. The intersection of regression line with the 0.2 mm offset line defines the J_{IC} value.

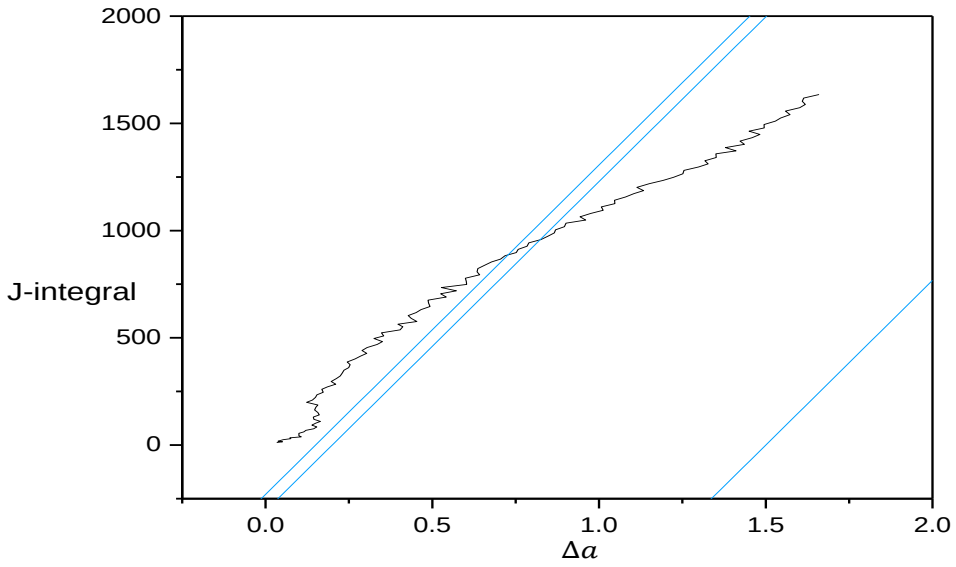

Fig 3.7: Identification of J_{IC} from J-R curve

Where,

A= Crack Extension

B= J-Integral

J_{IC} values are determine for different geometries at different temperature based on K_r and L_r values as described in above figure 3.7.

Chapter 4: FINITE ELEMENT SIMULATION

Finite element analysis includes three steps. The steps are processing, analysis and post processing. In our analysis, the processing includes the modelling of the specimen geometry. Boundary condition of the simulation like constraints, and displacements are applied by the Abaqus CAE tools. The CT specimen considered as three dimensional plane strain model. The material is considered as elastic plastic material and the properties of material like young's modulus, poison's ratio, yield strength are added in the model. The dimension of the specimen as considered in figure 4.1. Different types of modules are available in Abaqus CAE. Modules are used for the simulation and estimate the load-displacement values. With the help of this values, J-integral can be calculated which is used for the construction of level 3C FAD.

4.1 Finite element simulation for stationary crack growth

- Part Module –

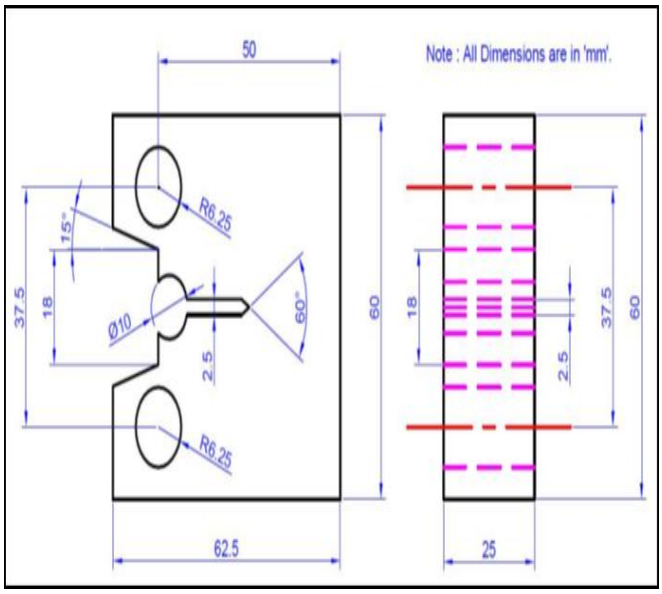

Fig 4.1: Schematic Diagram of CT Specimen

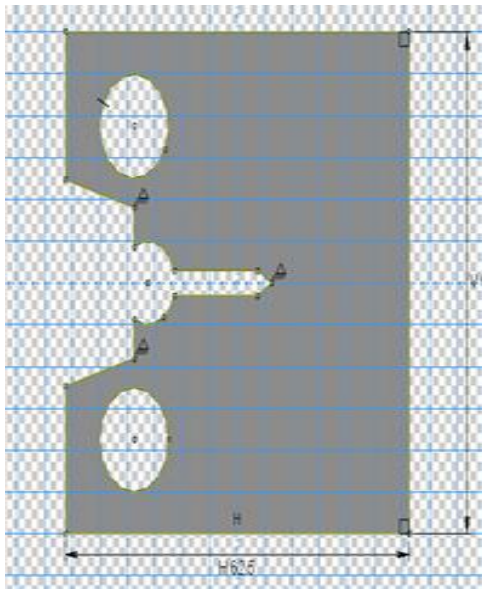

Fig 4.2: Sketch of a CT Specimen

Section sketch is the first step to create a model for the simulation. Many lines, curves and circles are drawn for the specimen dimensions. A depth value is given for thickness of the three dimensional model.

The loading pins are created as an analytical rigid body. Pins are not considered as the material of the model. Analytical rigid body does not require any material properties. Interaction between the pin and the specimen is defined as the surface to surface contact with the finite sliding formulation.

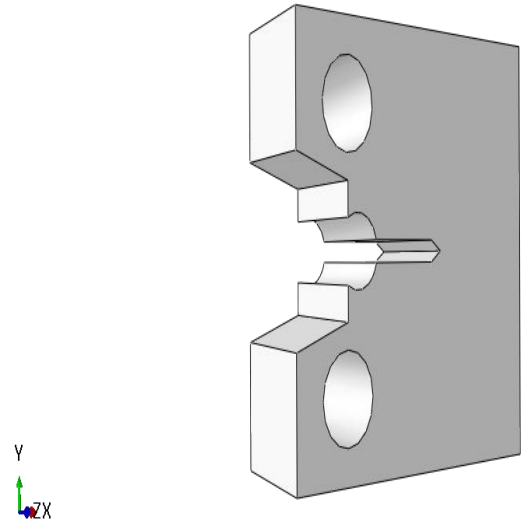

Fig 4.3: Three dimensional material model of CT specimen

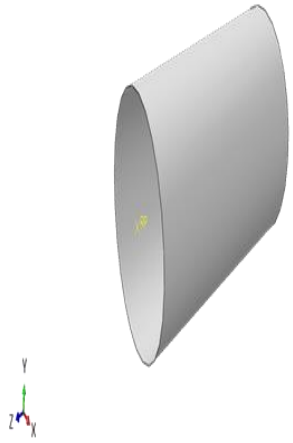

Fig 4.4: Three dimensional material model of pin

❖ Property Module-

- Create Material, Type = Isotropic, Elastic, Young's modulus = 210Gpa, Poisson's ratio =0.3
- Create Section, Homogeneous, Solid Section.
- Assign Section, Assign section to solid.

Elastic-Plastic material modelling can be done by adding Elastic and Plastic behaviour of material to the model. Material properties used as in the experimental material properties.

❖ Assembly Module –

- Instance Part, Choose Independent (Mesh on Instance)

❖ Step Module –

- Create Step, Static General
- Incrementation = Automatic
- Maximum number of increment = 100
- Increment size: Initial=0.01, Min=0.00001, max= 0.01

❖ Load Module –

- Create Load
- Point to the reference point in the pin
- Create Boundary Condition, Symmetry/Antisymmetry/Encastre,
- Select the plane
- Choose Pinned (U1,U2,U3)

Upper pin of the specimen is loaded vertically upward by the displacement of the pin from the reference point of pin. Two steps are created for the simulation:

Initial step is used to establish the contact between the pin and the specimen, this step is also used to constrain all the motion of the pin and specimen in all the direction. Next step is used for the loading of the upper pin. In the second step controlled loading of pin is applied.

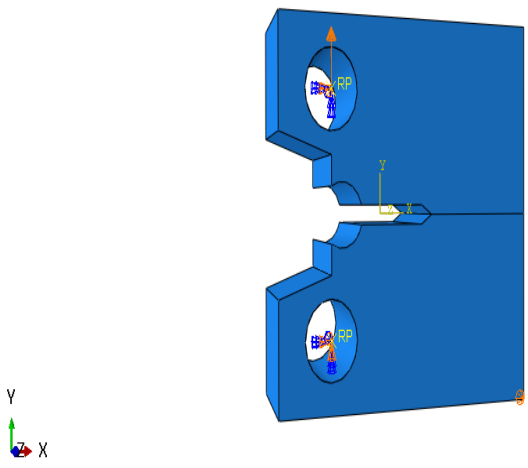

Fig 4.5: Boundary condition for material model

Interaction of the pin and specimen can be done by the interaction module of the Abaqus CAE. Last step before the simulation of model is meshing. This mesh generation is important

because material don't always have the same stresses at every point due to the loading. Meshing is basically a process which is creates some grid points called nodes. The results of the simulation are calculated by solving the relevant governing equations numerically at each of the nodes of the mesh.

- ❖ Mesh Module –

- ➢ Assign Mesh Control, Choose: Element Shape
- ➢ Seed Part Instance, Approximate Global Size = 0.0031,
- ➢ Mesh Part Instance

- ❖ Job Module –

- ➢ Create Job = Continue
- ➢ Job Manager = Submit
- ➢ When the analysis has completed, In the Job Manager = Results

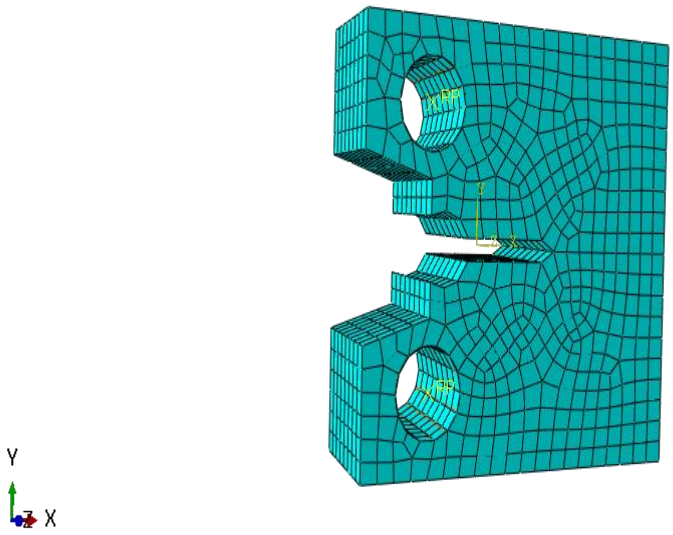

Fig 4.6: Mesh with element of the material model

After meshing, the Finite Element simulation is carried out of this CT specimen by using the Job module of the Abaqus CAE. Specimen deformed due to the upward vertical loading of the upper pin which is shown in figure 5.7.

❖ <u>Visualization Module –</u>

- Plot Contours on deformed Shape.
- In the Pull Down Menus choose: Result = Field Output = Choose a variable to visualize
- Animate Scale Factor
- Create XY data = ODB History output

A quick way to check the Reaction forces in your model is to initially plot the contours of the deformed shape. The default is S (Von Mises stress), It can be change from “S” to “RF” in the Visualization module. RF means “Reaction Forces”. This gives the range of the reaction forces of the model.

Create a new “History Output”. From the drop down menu, change the “Domain” from “Whole Model” to “Set”. Then select a predefined set created for the fixed nodes.

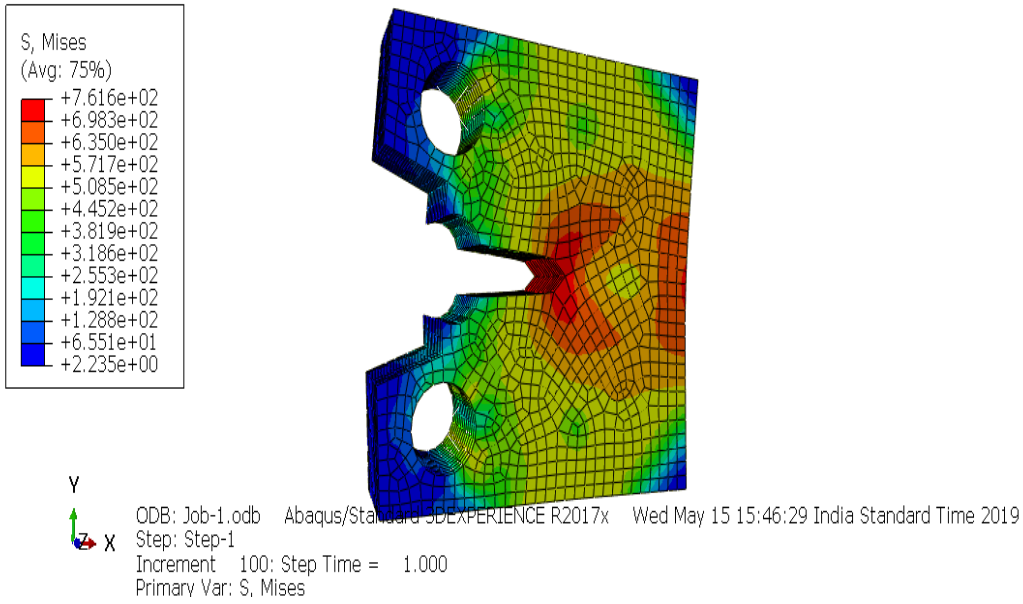

Fig 4.7: Result of Finite Element Simulation of the model

Reaction force and displacement of simulated model are required to collect. It can be obtain from a node that is subjected to displacement control, create a node-set for that node, which enable the calculation of reaction forces in field output requests for the particular set and obtain the reaction force on that node for each increment of the analysis.

Simulated Load-Displacement plot of a CT specimen is given below:

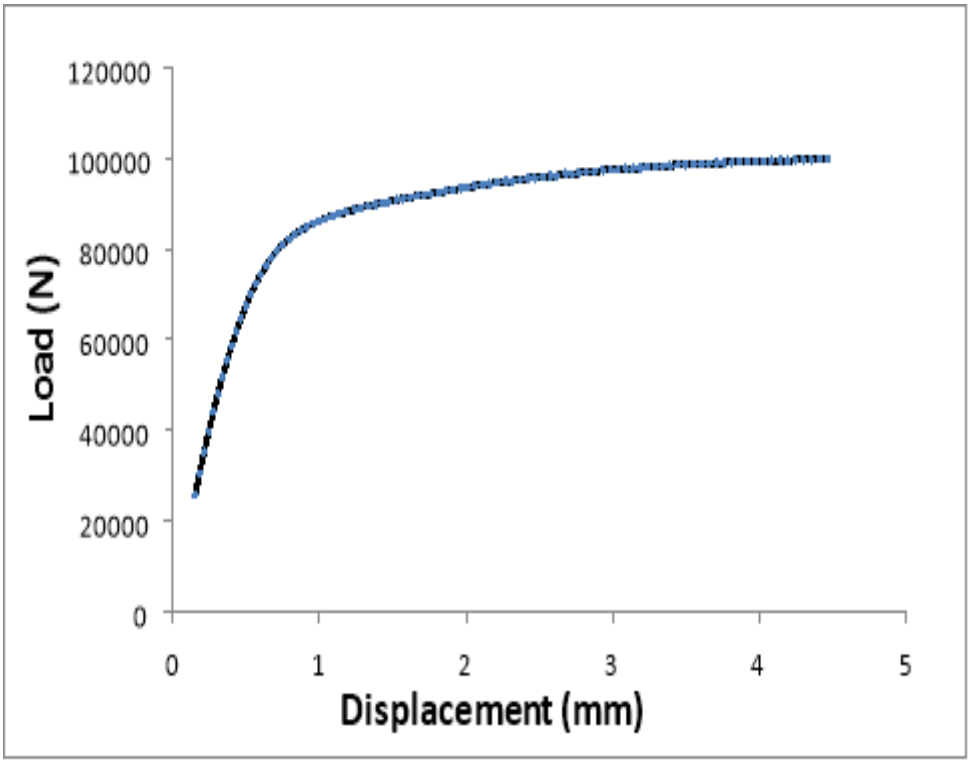

Fig 4.8: Simulated Load-Displacement curve

At first, the Load-Displacement data obtained from the finite element simulation are validated with the experimental Load-Displacement data as shown in figure 4.9 .

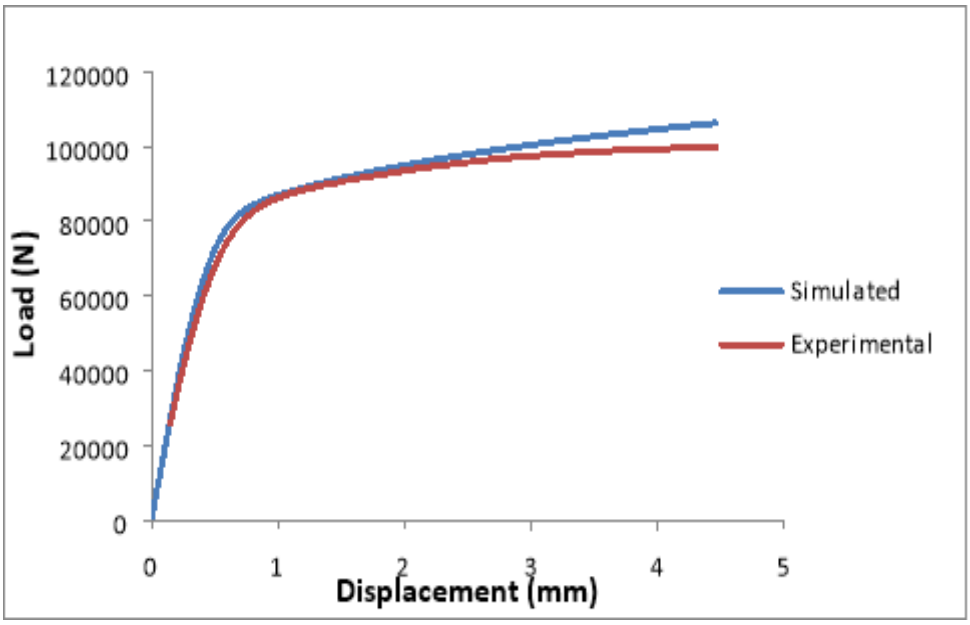

Fig 4.9: Experimental vs Simulated Load-Displacement Curve

It shows that Load-Displacement result of finite element simulation fairly match with the experimental Load-Displacement result. Then the result of finite element simulation can be used for the construction of Level 3C FAD from the empirical relationship as discussed in the chapter.

4.2 Calculation of J-Integral from Finite Element Simulation result

The calculation of J-integral from the load-displacement data according to the procedure described in ASTM E 1820 [21],

$$J_{total} = J_{el} + J_{pl} \tag{4.1}$$

Where,

The elastic J is computed from the elastic stress intensity:

$$J_{el(i)} = \frac{{K_{(i)}}^2(1 - v^2)}{E} \tag{4.2}$$

Where,

$J_{el(i)}$ = Elastic J-integral

K = Instantaneous stress intensity factor which is related to the current values of load and crack length.

$$K = \frac{P}{B\sqrt{W}} f\left(\frac{a}{W}\right) \tag{4.3}$$

Where,

P - Applied load

B - Thickness of the specimen

W - Width of the specimen

f(a/W) - Dimensionless geometry function for a compact tension specimen

where,

f(a/W) for a compact tension specimen is given below,

$$f\left(\frac{a}{W}\right) = \frac{2+\left(\frac{a}{W}\right)}{(1-(a/W))^{\left(\frac{3}{2}\right)}}\left[0.886 + 4.64\left(\frac{a}{W}\right) - 13.32\left(\frac{a}{W}\right)^2 + 14.72\left(\frac{a}{W}\right)^3 - 5.60\left(\frac{a}{W}\right)^4\right] \quad (4.4)$$

The basic procedure in ASTM E 1820 [21] includes a simplified method for computing J_{pl} from the plastic area under the load displacement curve,

$$J_{pl(i)} = \left[J_{pl(i-1)} + \left(\frac{\eta}{Bb_0}\right)\frac{\left(P_i + P_{(1)}\right)\left(\Delta_{i(pl)-}\Delta_{i-1(pl)}\right)}{2}\right] \quad (4.5)$$

$$\eta = 2 + 0.522\left(\frac{b_0}{W}\right) \quad (4.6)$$

Where,

$J_{pl(i)}$– Plastic J computed from the area under load-displacement curve at each time increment.

P_i– Load at each time increment.

P_1 – Initial Load

$\Delta_{i(pl)-}$– Plastic displacement at each time increment.

B – Net thickness of the specimen

$b_{(0)}$– Initial Un-cracked ligament length.

η – Dimensionless constant.

a – Initial Crack Length

The calculated values of J-integral for both the experimental and simulation can be validated in terms of J-R curve as shown in the figure 6.2

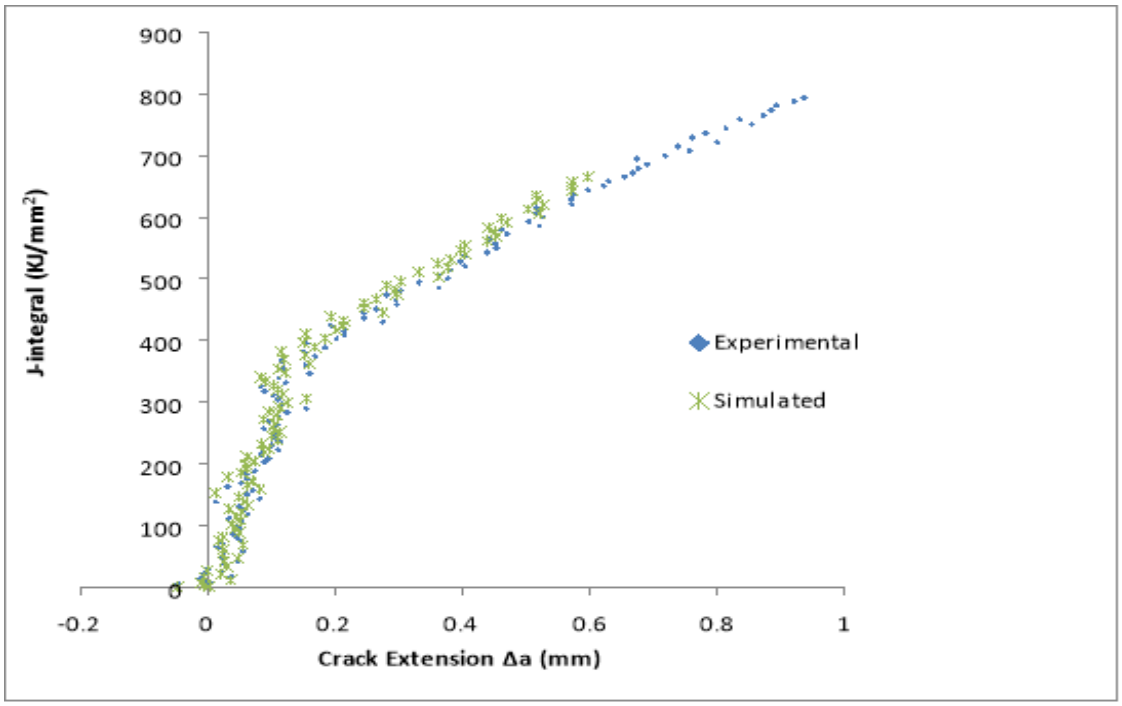

Fig 4.10: J-R curve of CT specimen (Experimental vs Simulation)

The above figure shows that the simulated result extracted from Finite Element Simulation is fairly match with the Experimental result.

So, the result of simulation can be used for the construction of the level 3C Failure Assessment Diagram for different a/W at different temperature with the parameter(Kr and Lr) as discussed in the earlier,

Chapter 5: DEVELOPMENT OF DIFFERENT LEVELS OF FAD

5.1 FAD curve option-

The most rigorous method to determine a Failure Assessment Diagram curve for a particular application is to perform an elastic-plastic J-integral analysis and define Lr and Kr. Such an analysis can be complicated. So, simplified approximations of FAD curve are available.

The Central Electricity Generating Board in UK incorporated the strip yield failure assessment into a fracture analysis methodology, which is known as the R6 approach [3] and various changes are made further. The options are described in the BS 7910(2005).The options are given below:

5.1.1Option: Level 3A FAD

The empirical relationship of Level 3A FAD,

$$K_r = \left[1 + 0.14\left(L_r{}^2\right)\right]\left\{0.3 + 0.7\exp\left[-0.65\left(L_r{}^6\right)\right]\right\} \quad (5.1)$$

The above equation 5.1 is valid only when the stress-strain data are not available for the material and the above equation assume that the FAD is independent of both the material properties and geometry.

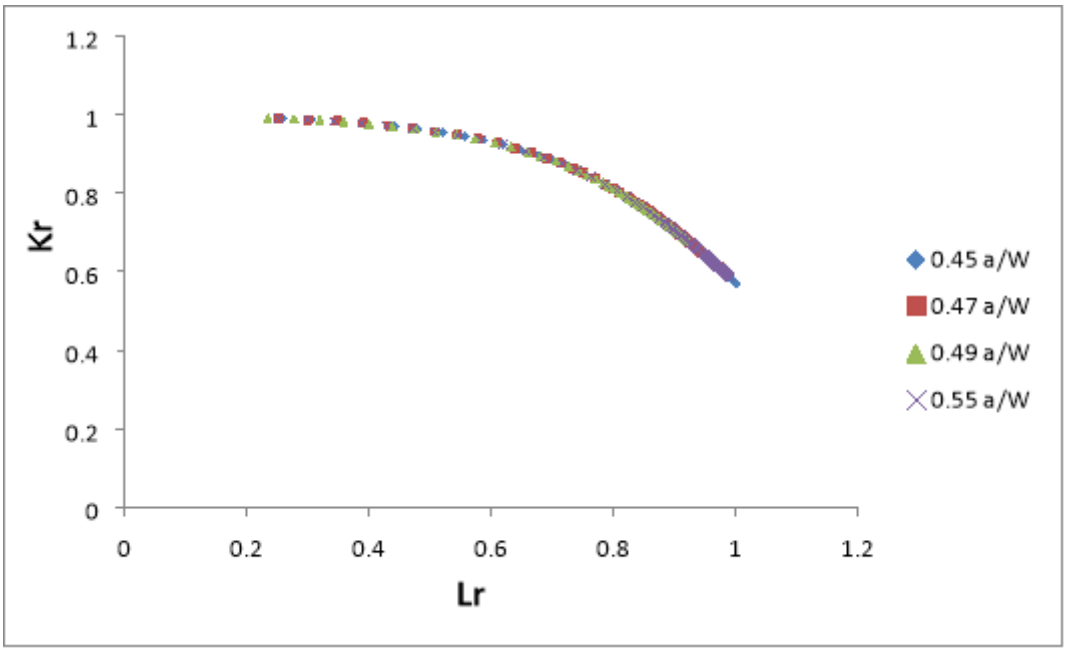

Fig 5.1: Level 3A FAD for different a/W

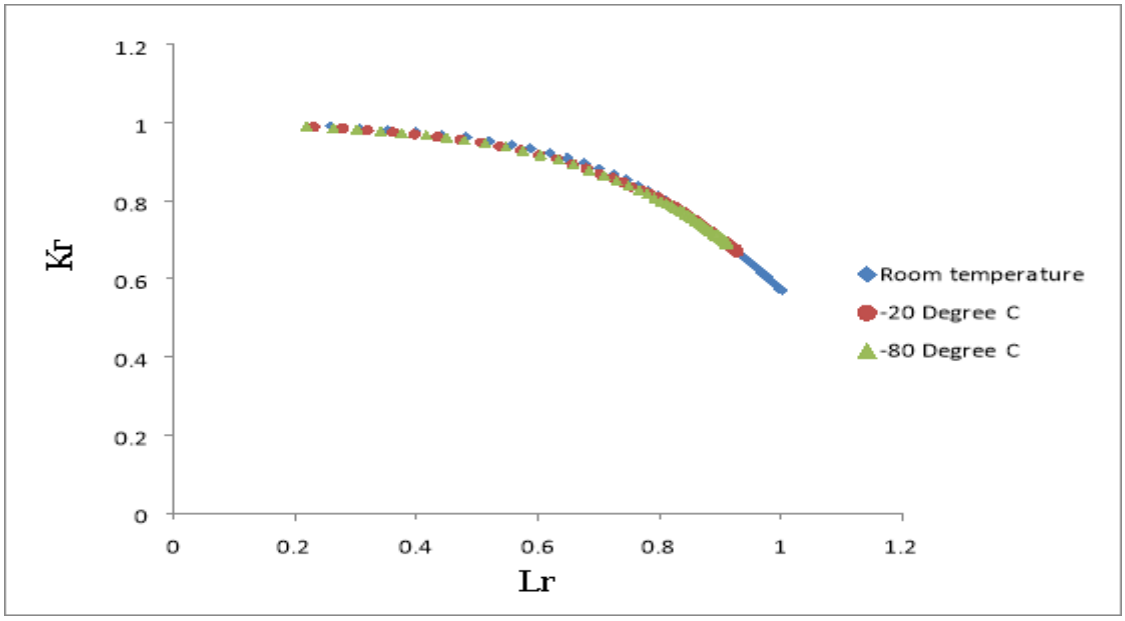

Fig 5.2: Level 3A FAD on different temperature

Since, the level 3A FAD is material independent and geometry independent, it shows that Level 3A FAD is same for each every material and geometry at different temperature as shown in figure 5.1 and 5.2.

5.1.2 Option: Level 3B FAD

The empirical relationship of Level 3B FAD,

$$K_r = \left[\left(1 + \alpha {L_r}^{n-1}\right) + \frac{{L_r}^2}{\left(1 + \alpha {L_r}^{n-1}\right)}\right]^{-1/2} \quad (5.2)$$

It can be described from the above figure 5.3 that level 3B FAD is dependent on material property where α and n are the Ramberg-Osgood parameters as discussed earlier. The values of α and n are determined for different temperatures from the tensile stress-strain data. It is seen that the values of n decrease with the decreasing temperature. As seen from figure 3.3, it was earlier observed that the material did not lose its ductility with deceasing temperature. This may be probably due to addition of nickel in the material. As determined from tensile stress-strain data the level 3B FAD curve obtained using the tensile properties show that the contribution of plastic collapse for the failure of material is more dominant as compared to brittle phenomenon.

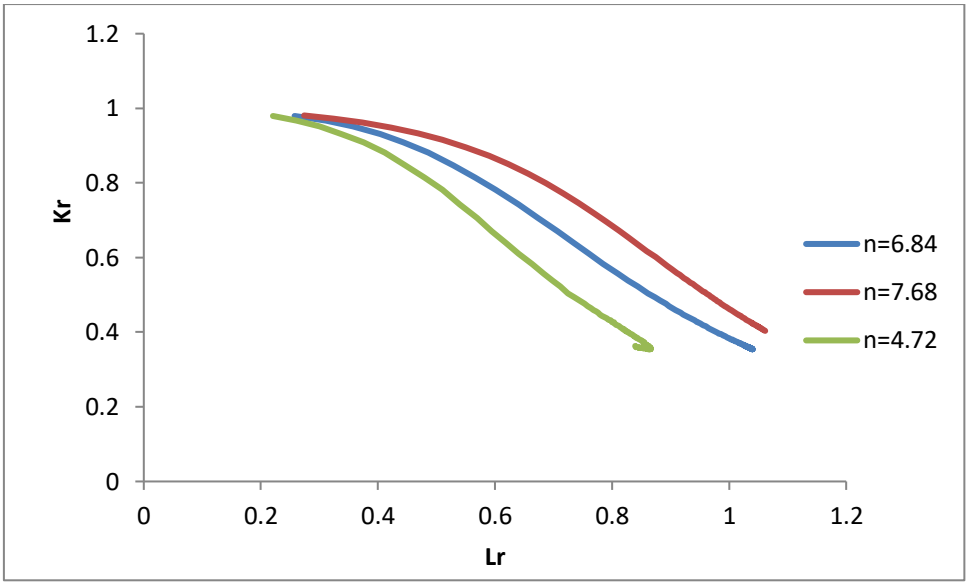

Fig 5.3: Level 3B FAD for different n values

5.1.3 Option: Level 3C FAD –

Finite element simulations are carried out for each and every components individually so both the material properties and geometry of the component is consider in level 3C FAD. It is already discussed.

Different CT specimen geometry with different a/w ratio and at different temperature conditions are simulated. This results of finite element simulation are used for the construction of level 3C FAD.

Once the load-displacement result of simulation and experimental result are validated then the failure assessment diagram is constructed for different specimen at different temperature in terms of two parameters (K_r and L_r). Simulated Load-displacement results are used for the calculation of J-integral. The calculation of J-integral from the simulated load-displacement data is given below,

Finite element simulations are carried out for the each and every model individually. So, both the properties of the model are taken into consideration. Therefore, level 3C FAD is determined from the elastic-plastic finite element analysis result to consider material properties and geometry properties.

K_r and L_r values are calculated from the Finite element simulation data and used to construct the level 3C FAD.

$$K_r = \sqrt{\frac{J_{el}}{J_{total}}} = \frac{K_I}{K_J} \tag{5.3}$$

$$L_r = \frac{P}{P_0} = \frac{\sigma_{ref}}{\sigma_{ys}} \tag{4.4}$$

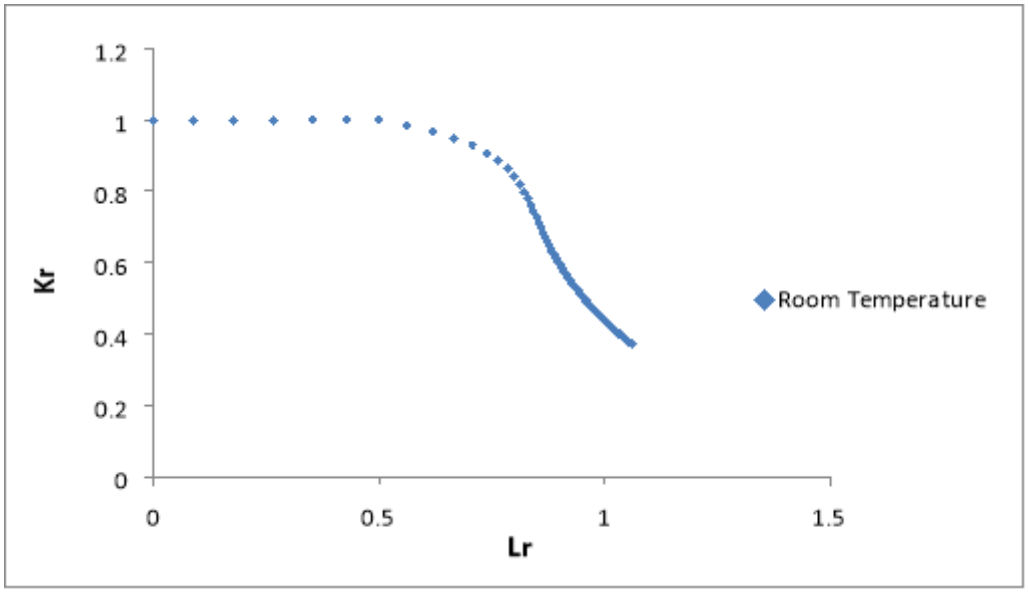

Fig 5.4: Level 3C FAD at room temperature

5.2 Effect of temperature on level 3C FAD

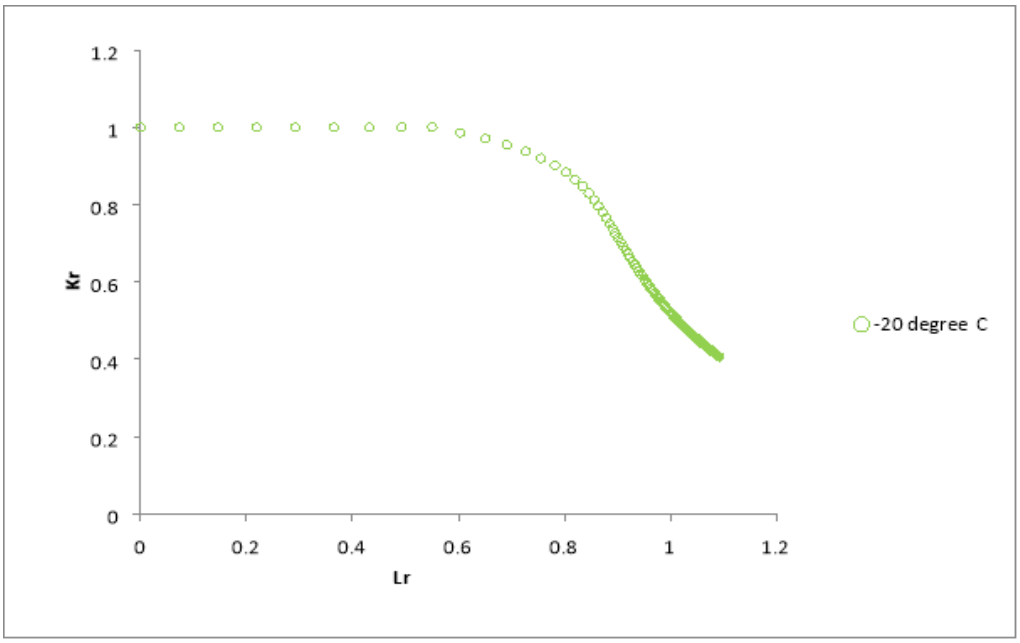

Fig 5.5: Level 3C FAD at -20 degree C Temperature

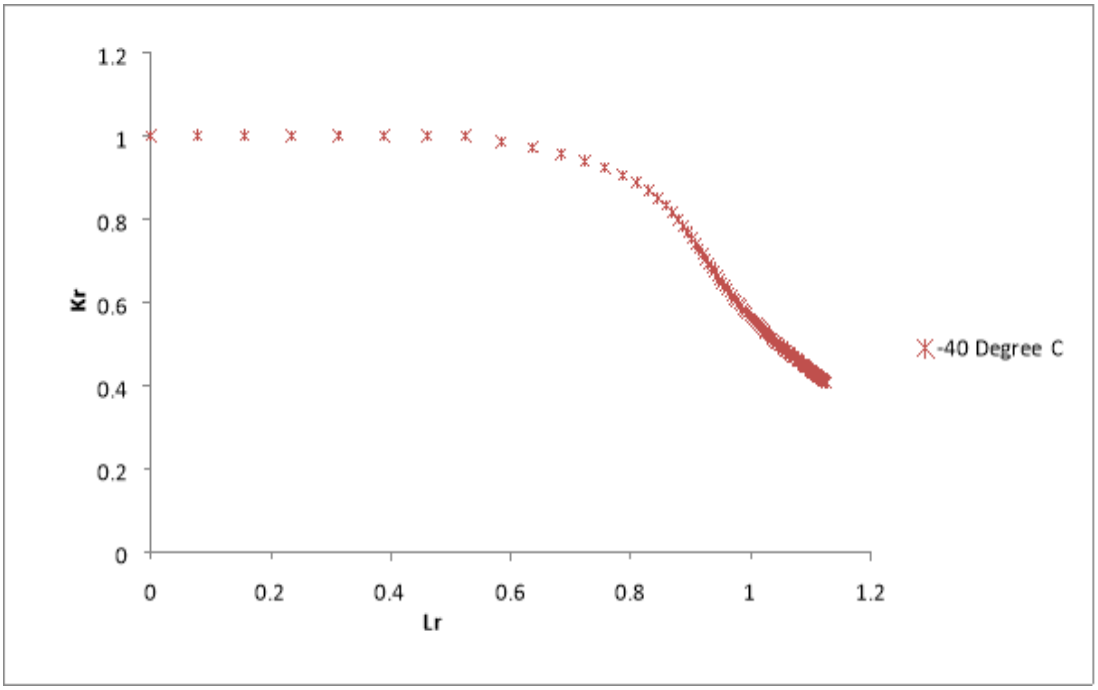

Fig 5.6: Level 3C FAD at -40 degree C Temperature

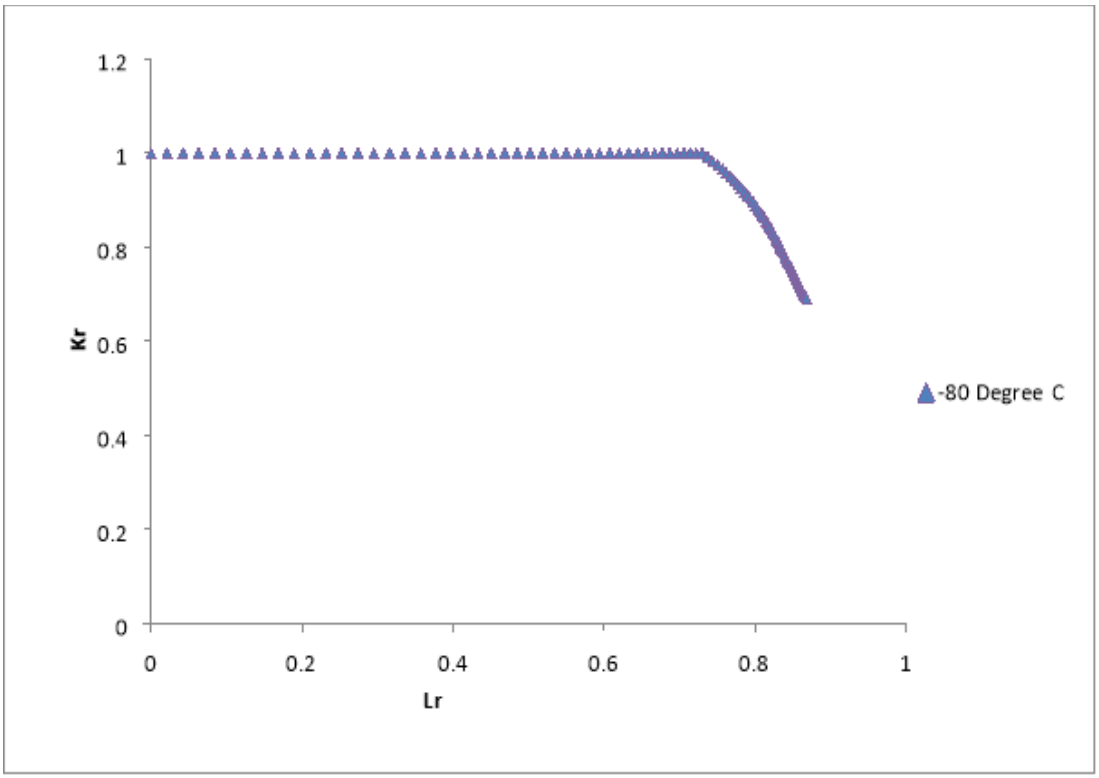

Fig 5.7: Level 3C FAD at -80 degree C Temperature

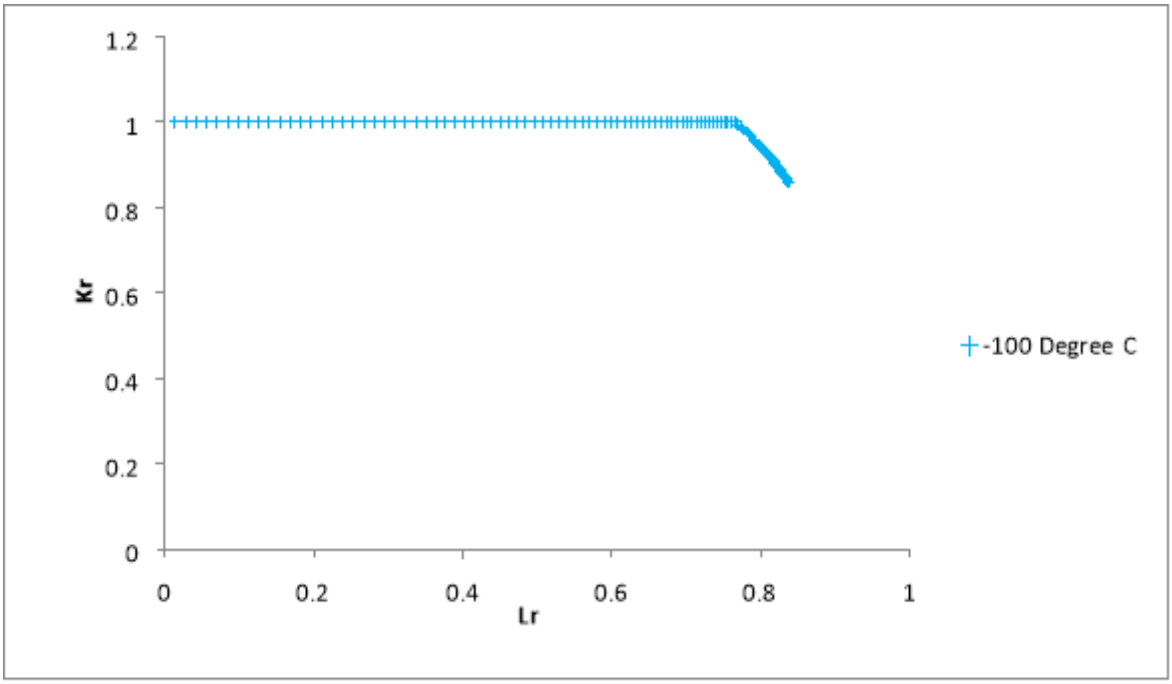

Fig 5.8: Level 3C FAD at -100 degree C Temperature

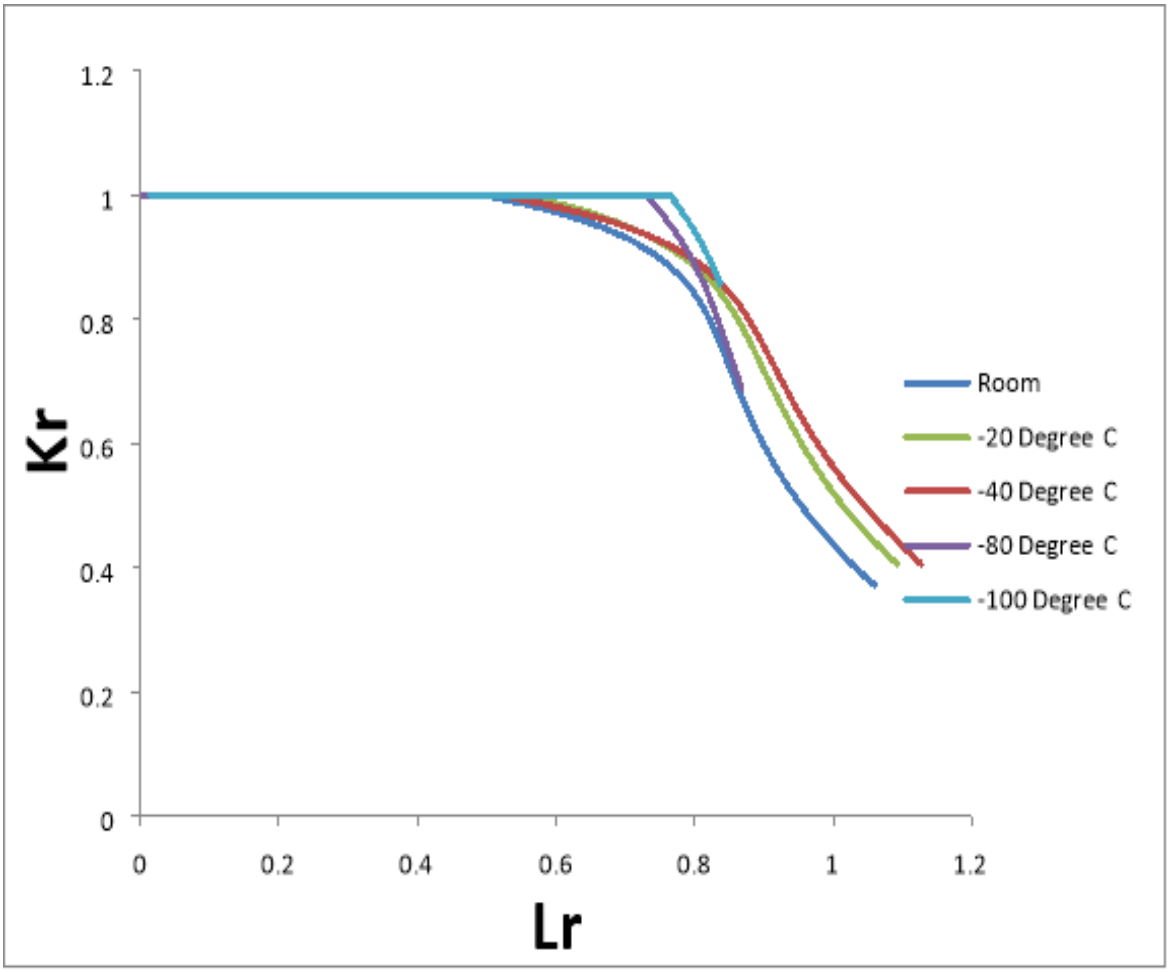

Fig 5.9: Level 3C FAD at different Temperature

Temperature	Lr Value	Kr Value
Room Temperature	0.56	0.98
-20^0 C	0.60	0.98
-40^0 C	0.636	0.97
-80^0 C	0.743	0.98
-100^0 C	0.772	0.98

Table 3: K_r and L_r values at point where value of K_r drops from 1.

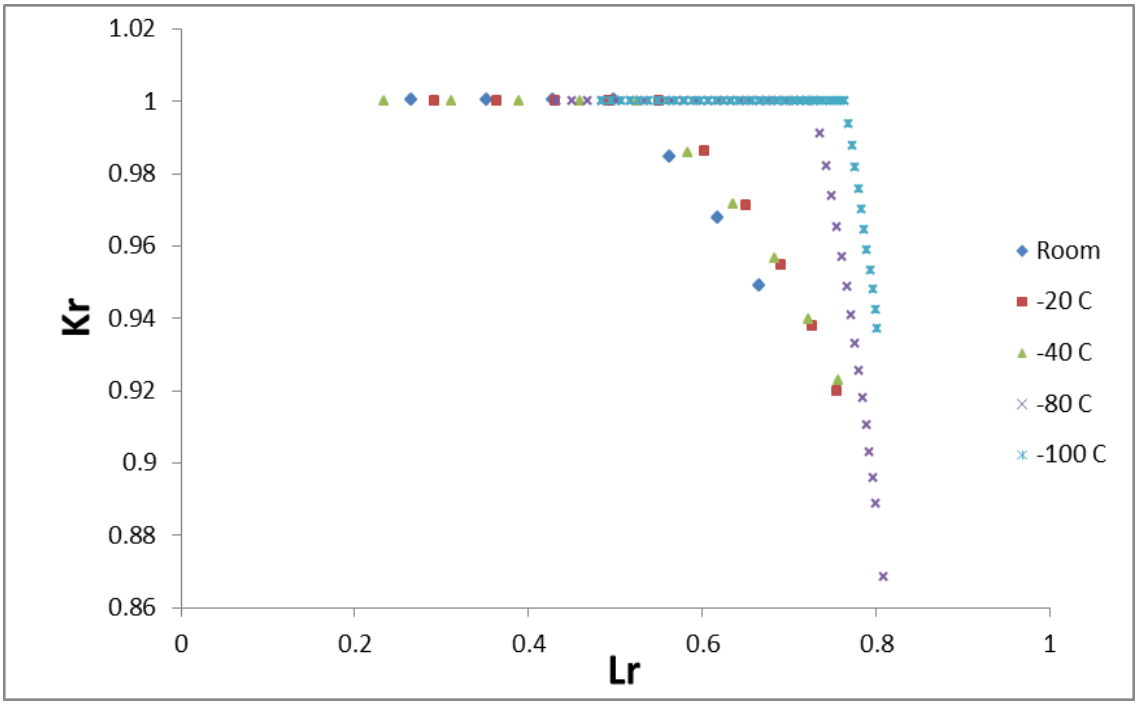

Fig 5.10: Enlarge view of level 3C FAD where it departs from the brittle fracture line at different temperature

Level 3C FAD curve obtained using three dimensional elastic-plastic finite element analysis results and it shows clearly in above figures that the locus of curve differ at lower temperature than room temperature. In general, ductility of material decreases with decrease in temperature. Figure5.10 shows that as the temperature decreases FAD curve indicates that the brittle nature of failure is dominant compared to plastic collapse. This is nothing but a clear indication of loss of ductility of material at lower temperature. The above phenomenon was not captured in level 3B FAD because the values of n and α did not signify loss of ductility based on tensile experimental results.

At room temperature, the value of L_r is 0.56 where the FAD curve shifts perfectly brittle failure phenomenon (i.e. K_r=1 as shown in *Table 3*). Similarly the values of L_r for different temperature is plotted which is shown in *Table 3*. It is inferred from the table 3 that the contribution of material subjected to failure gradually shift towards perfectly brittle phenomenon with decreasing temperature.

Temperature of the material is a factor that determines whether it fails as brittle in nature or as plastic collapse. Temperature is a factor which is reflects in Level 3C FAD curve can be observed as shown in above figures.

Chapter 6: CONCLUSION

6.1 Closing Remarks

[1] The level 3A FAD obtained using the equation 5.2 as discussed in earlier chapter. It is independent of geometry and material properties as shown in figure 5.2 and figure 5.3. It cannot consider hardening effect in it. So, a material specific FAD curve is required.

[2] The level 3B FAD obtained using the equation 5.6 and it shows material property dependence curve. The values of Ramberg-Osgood parameter like α and n determines the nature of FAD curve. As shown in figure 5.7, the value of n decrease there is a more gradual tail in FAD. However the level 3B FAD does not take into account the geometry dependence.

[3] Finite element simulation results are used to obtain the level 3C FAD curve and it shows both the geometry and material dependence as shown in figure. It is observed that as the temperature decreases the curve of FAD shifts more towards the contribution of brittle factor. The loss in ductility increases with the decrease in temperature which reflects in the Level 3C FAD.

[4] The values of L_r and K_r on FAD curve at the point where it departs from the brittle fracture line (plasticity level at failure point) for different temperatures have been listed in the Table number 3. It can be inferred from this table that the value of K_r drops from 1 at a higher value of L_r with decrease in temperature showing higher brittleness. The value of K_r drops from 1 with the L_r value of 0.56 at room temperature whereas value of K_r drops from 1 with a higher L_r value of 0.63 at -40 degree C. It follows the trend up to -100 degree C where the value of L_r is 0.77 as shown in table number 2. It signifies that the contribution of brittle factor is more apparent with decrease in temperature which was not apparent in tensile curves.

[5] It is established from the present study that FAD (level 3C) is not only an effective tool to predict the failure point considering both the effects of crack growth and plasticity. It also captures the effect of temperature on shift of failure point due to loss of ductility.

6.2 Future Scope

[1] J-Integral values can be predicted from the level 3A Failure Assessment Diagram curve at different temperature.

[2] Estimation of failure load at component level with variation in temperature from J-R curve and Load-Displacement curve.

References

1) **Burdekin, F.M. and Dawes, M.G.,** "Practical Use of Linear Elastic and Yielding Fracture Mechanics with Particular Reference to Pressure Vessels." Proceedings of the Institute of Mechanical Engineers Conference, London, May 1971, pp. 28–37
2) **Dowling, A.R. and Townley, C.H.A.,** "The Effects of Defects on Structural Failure: A Two-Criteria Approach." International Journal of Pressure Vessels and Piping, Vol. 3, 1975, pp. 77–137.
3) **Harrison, R.P., Loosemore, K., Milne, I., "**Assessment of the Integrity of Structures Containing Defects." CEBG Report R/H/R6, Central Electricity Generating Board, UK, 1976.
4) **Bloom, J.M.,** "Prediction of Ductile Tearing Using a Proposed Strain Hardening Failure Assessment Diagram." International Journal of Fracture, Vol. 6, 1980, pp. R73–R7.
5) **PD 6493:1980**, "Guidance on Some Methods for the Derivation of Acceptance Levels for Defects in Fusion Welded Joints." British Standards Institution, London, March 1980.
6) **Shih, C.F., German, M.D., and Kumar, V.**, "An Engineering Approach for Examining Crack Growth and Stability in Flawed Structures." International Journal of Pressure Vessels and Piping, Vol. 9, 1981, pp. 159–196.
7) **Ainsworth, R.A.,** "The Assessment of Defects in Structures of Strain Hardening Materials." Engineering Fracture Mechanics, Vol. 19, 1984, p. 633-642.
8) **Bradford R., Gates R.S., Green G., Williams D.C.**, "A Strain Hardening Failure Assessment Diagram derived from Carbon-Manganese Steel Compact Tension Specimens" International Journal of Pressure Vessels and Piping, Vol. 19, 1984, pp. 83–99.
9) **Milne, I., Ainsworth, R.A., Dowling, A.R., and Stewart, A.T.,** "Background to and Validation of CEGB Report R/H/R6—Revision 3." International Journal of Pressure Vessels and Piping, Vol. 32, 1988, pp. 105–196.

10) **Needleman A., "**AN ANALYSIS OF TENSILE DECOHESION ALONG AN INTERFACE" Journal of Mechanics and Physics of solid,Vol.38, No. 3, pp. 289-324,1990.
11) **BS PD 6493**," Guidance on methods for assessing the acceptability of flaws in fusion welded structures. British Standards Institution, London, 1991.
12) **Tvergaard Viggo** and **Hutchinson W. John**. ,"The relation between crack growth resistance and fracture process parameters in elastic-plastic solids." Journal of Mechanics and Physics of solid,Vol.40, No. 6, pp. 1377-1397,1992.
13) **BS 7970:1999**, "Guidance on Methods for Assessing the Acceptability of Flaws in Metallic Structures." Amendment No. 1, British Standards Institution, London, 2000.
14) **Friedman Edward** and **Wilson Williams K.,** "Stress Intensity Factor Plasticity Correction for Flaws in Stress Concentration Regions" Bechtel Bettis, Inc. Bettis Atomic Power Laboratory West Mifflin, PA.
15) **Budden P.J**.," Failure assessment diagram methods for strain-based fracture" Engineering Fracture Mechanics, Vol. 73 pp.537–552, 2006.
16) **Tipple C.** and **Thorwald G. "** Using the Failure Assessment Diagram Method with Fatigue Crack Growth to Determine Leak-before-Rupture**"** Simulia Customer Conference 2012.
17) **Marcos A. Bergant., Alejandro A. Yawny., Juan E. Perez Ipina**. "Failure Assessment Diagram in Structural Integrity Analysis of Steam Generator Tubes".International Congress of Science and Technology of Metallurgy and Materials, SAM -CONAMET 2013
18) **Ilkka Valkonen. "**Estimation of limit load capacity of structural steel with yield strength 960 MPa." Weld World (2014) 58:839–852
19) **Sang-Hyun Kim, Jae-Min Gim, Wang Miao, Yun-jae Kim**. "Simplified limit load estimation using m-tangent method for branch pipe junctions under internal pressure and in-plane bending." 21st European Conference on Fracture, ECF21, 20-24 June 2016.
20) **ASTM E8/E8M**-11 Standard Test Methods for Tension of Metallic Materials.
21) **ASTM1820 -11E1** Standard Test Method for Measurement of Fracture Toughness.
22) **ASTM E647-11E1** Standard Test Method for Measurement of Fatigue Crack Growth.
23) **ASTM E813-81** Standard Test Method forJ_{IC}, a Measure of Fracture Toughness.